Synthesis and Characterization of Mn doped ZnO for Thermistor Application

M.Tech. Thesis

By

SHUBHAM CHOUDHARY

DISCIPLINE OF METALLURGY ENGINEERING & MATERIALS SCIENCE

INDIAN INSTITUTE OF TECHNOLOGY INDORE

JUNE 2019

Synthesis and Characterization of Mn doped ZnO for Thermistor Application

A THESIS

Submitted in partial fulfillment of the requirement for the award of the degree

of

Master of Technology

by

SHUBHAM CHOUDHARY

DISCIPLINE OF METALLURGY ENGINEERING & MATERIALS SCIENCE

INDIAN INSTITUTE OF TECHNOLOGY INDORE

JUNE 2019

INDIAN INSTITUTE OF TECHNOLOGY INDORE

CANDIDATE'S DECLARATION

I hereby certify that the work which is being presented in the thesis entitled **SYNTHESIS AND CHARACTERIZATION OF Mn DOPED ZnO FOR THERMISTOR APPLICATION** the partial fulfillment of the requirements for the award of the degree of **MASTER OF TECHNOLOGY** and submitted in the **DISCIPLINE OF METALLURGY ENGINEERING AND MATERIALS SCIENCE, Indian Institute of Technology Indore**, is an authentic record of my own work carried out during the time period from July 2017 to June 2019 under the supervision of Dr. Parasharam Shirage, Associate Professor and Dr. Dhirendra Kumar Rai, Assistant Professor, Discipline of Metallurgy Engineering and Materials Science, Indian Institute of Technology, Indore.

The matter presented in this thesis has not been submitted by me for the award of any other degree of this or any other institute.

Signature of the student with date
SHUBHAM CHOUDHARY

This is to certify that the above statement made by the candidate is correct to the best of my/our knowledge.

Signature of the Supervisor of M.Tech. thesis (with date)
Dr. PARASHARAM SHIRAGE

Signature of the Co-Supervisor of M.Tech. thesis (with date)
Dr. DHIRENDRA K RAI

SHUBHAM CHOUDHARY has successfully given his/her M.Tech. Oral Examination held on **26/06/2019**.

Signatures of Supervisors of M.Tech. thesis
Date:

Convener, DPGC
Date:

Signature of PSPC Member #1
Date:

Signature of PSPC Member #1
Date:

ACKNOWLEDGMENTS

First and foremost, I would like to express my most indebt gratitude to my supervisor **Dr. Parasharam M. Shirage** for his continuous guidance, support, and encouragement during the course of my research. The whole of this work is carried out under his guidance. His wide research experience and expertise in the subject helped me in understanding scientific topics at a deeper level. I also thank them for his trust in me and for giving me a lot of freedom to try new ideas. Also, I am thankful to my co-supervisor **Dr. Dhirendra Kumar Rai** for his timely advice.

I express my sincere thanks to **Prof. Pradeep Mathur (Director, IIT Indore)**, who has been very encouraging during the entire course of my master's work. I also convey sincere thanks to **Dr. Rupesh Devan** and **Dr. Amrendra Kumar Singh** for their support and motivation and for taking time to be my PSPC member and review and evaluate my work.

I am also grateful to **Sophisticated Instrumentation Centre (SIC), IIT Indore** for providing characterization facility and the staff for cooperation.

I would also like to take this opportunity to thank my labmates from **Advance Functional Material Research Group, IIT Indore (AFMRG)** for their company and being supportive all the time. A special thanks to **Dr. Prateek Bhojane** and **Mr. Alfa Sharma** for their technical expertise and many discussions, which proved invaluable to the work in this thesis and also like to acknowledge their willingness to help, and especially with the setting up of experiments and their patience in answering all my questions.

Above all, the credit goes to all my **Bachelors and Masters Friends**, who instigated the will to believe in myself and impelled me to pursue my dreams and became an imploring companion in this journey and for the Odyssey yet to come. Their profound knowledge and an optimistic attitude always imparted a focus to strengthen the fundamentals and encouraged me to ascent towards excellence. Last, but not the least, I express my endearing gratitude to my **Family** for their

unconditional love, support and patience that enabled me to achieve my goals and I dedicate this thesis to them.

Abstract

Doping of Zinc Oxide with Manganese has been done to study the effect of Mn on ZnO properties. Syntheses of samples were done using a simple, easy and cheap Wet chemical approach to reduce growth dependent variables like high pressure, high temperature, etc. Samples were synthesized on a glass substrate to make the process more economical. Atomic fraction of Mn is changed to study its effect on $Zn_{1-x}Mn_xO$ nanostructures (x= 0%, 5%, 7.5%, 10%, 12.5%). Structural properties of the samples have been studied using X-Ray Diffraction method and Raman Spectroscopy; Morphological study has been done using FESEM; Optical property has been studied using UV Vis spectroscopy and Photoluminescence spectroscopy. These studies depict that Mn doping changes the morphology of ZnO nanostructure from nanoflowers to nanorods with a reduction in diameter. Nanorods preferred to grow in (002) plane, while the lattice parameter, unit cell volume, and bond length increased with Mn doping. Raman spectra show an extra peak for Mn in ZnO. PL study depicted the formation of defects in ZnO nanostructure due to vacancy, interstitial, and antisite defects. Temperature sensing application of Mn doped ZnO is done and the device found to be an NTC resistor and the sensitivity of the device increased with Mn doping.

TABLE OF CONTENTS

Chapter 3: Characterization Technique 18-26

Chapter 4: Experimental Method and Material 27-32

Chapter 5: Result and Discussion 33-48

LIST OF FIGURES

LIST OF TABLES

NOMENCLATURE

A	Ampere
C	Carbon
Cu	Copper
CB	Conduction band
CBD	Chemical bath deposition
CVD	Chemical Vapour deposition
DI	Deionized water
DMS	Dilute magnetic semiconductor
E_g	Energy gap
FESEM	Field emission scanning electron microscopy
FTO	Fluorine doped tin oxide
H	Hydrogen
ITO	Indium tin oxide
K	Kelvin
M	Molarity
Mn	Manganese
NTC	Negative Temperature Coefficient
O	Oxygen
PL	Photoluminescence
PTC	Positive Temperature Coefficient
PMT	Photo Multiplier Tube
RT	Room temperature
SEM	Scanning electron microscopy
TCR	Temperature Coefficient of Resistance
UV	Ultraviolet
Vis	Visible
VB	Valence band
V	Voltage
XRD	X-Ray diffraction
Zn	Zinc

Physical Constants and Conversion Factors

Avogadro's number	NA = 6.02×10^{23} molecules/mole
Boltzmann's constant	$k = 1.38 \times 10^{-23}$ J/K, 8.62×10-5 eV/K
Electronic charge	$q = 1.6 \text{ x } 10^{-19}$ C
Planck's constant	$h = 6.63 \times 10^{-34}$ J.s, 4.14×10^{-15} eV.s
Speed of light	$c = 3 \times 10^{8}$ m/s, 3×10^{10} cm/s

CHAPTER 1

INTRODUCTION

1. Nanotechnology

A field with tremendous growth and potential to generate novel materials having varying properties, thus giving a vast approach to discover, innovate and solve questions of fabrication of a device. Nanotechnology has already been used efficiently and effectively in electronics, automobiles, beauty products, bio-medicine, etc. and has touched all fields of human life fulfilling all their needs.

In 1974 a Japanese scientist Norio Taniguchi coined the term ”Nanotechnology” **[1]**. the famous talk of Richard Feynman “There’s Plenty of Room at the Bottom” in 1959 highlighted the need of innovating, controlling and manipulating materials at the nano level **[2]**. .In 80s decade various characterization tools were invented which helped to study nanomaterial. Since then nanotechnology has nearly grasped all fields of human discovery and fulfilled the needs of generations of living beings.

2. Nanomaterial

Size plays an important role in altering the properties of a material. Synthesis of a material having controlled growth of at least one dimension to be less the 100 nm is termed as Nanomaterial. These materials exhibit different properties from there bulk material because as the size of material in any direction is reduced, the surface area to volume ratio increases and then material properties are dependent on surface properties. Research and Development in the field of nanomaterial in past has produced many nanostructures as nanoflowers, nanorods, quantum dots, nanowires, nanoflakes, nanosheets, nanotubes, etc. as can be seen from Figure 1.1 **[3].**

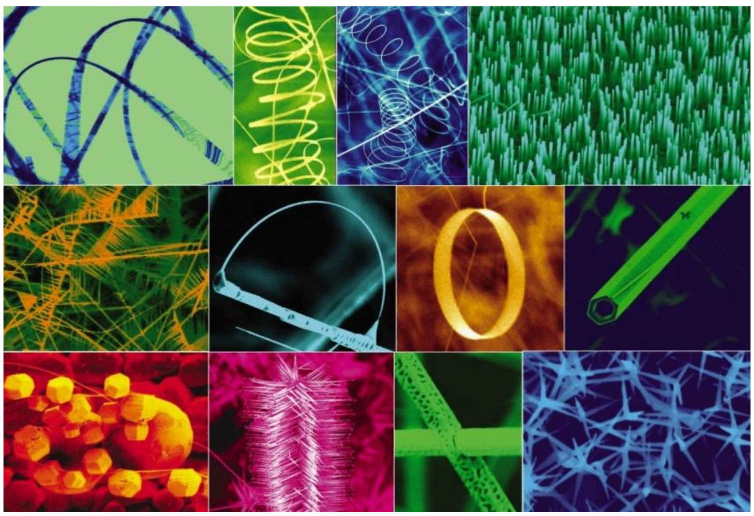

Figure 1.1. Different types of Nanostructures. **[3]**

- **Types of nanostructure of materials [4]**

  - **0 D (Zero dimensional)**

    These Nanostructures have all three dimensions less than 100 nm, like quantum dots

- **1 D (One Dimensional)**

  These Nanostructures have any 2 dimensions less than 100 nm and grow only in 1 dimension, like nanorods.

- **2 D (Two Dimensional)**

  These Nanostructures have only 1 dimension less than 100 nm and grow in other 2 dimensions, like nanosheets.

3. Zinc Oxide (ZnO)

An inorganic compound, which is available in nature as mineral Zincite, containing impurities like manganese gives it a yellowish red color. Pure ZnO is white in color and is insoluble in water. ZnO is chemically stable, nontoxic, biocompatible, anti-corrosive, anti-bacterial, and anti-microbial having semiconducting, piezoelectric properties used in day to day life of human interaction. ZnO material accounts a large number of nanostructure depending upon synthesis techniques, time, temperature and precursor used, distinct varieties of nanostructure also helped ZnO material to possess different material properties with different nanostructures. Nano-ZnO market trend shows a tremendous rise in recent years and expected to double its market production until 2022 with a high share in rubber and cosmetic industries **[5]**.

❖ Crystal Structure:

ZnO possesses 3 crystal structures Wurtzite, Zinc-Blende, Rocksalt (or Rochelle salt) as shown in figure 1.2. Zinc Wurtzite structure is most widely found and thermodynamically stable [6]. This wurtzite structure has a Zn^{2+} anion which is surrounded by 4 O^{2-} cation or vice versa by an sp3 covalent bonding at the corner of the tetrahedron as can been seen from figure 2. ZnO has partly ionic bond due to its Zn-O ionic character and partly covalent bond, largely ionic with corresponding ionic radii 0.074nm of Zn^{2+} and 0.140nm of O^{2-}ions. Zinc Blende structure growth stabilizes on cubic lattice structure while the Rocksalt structure needs high pressure about 10 GPa for growth [7].

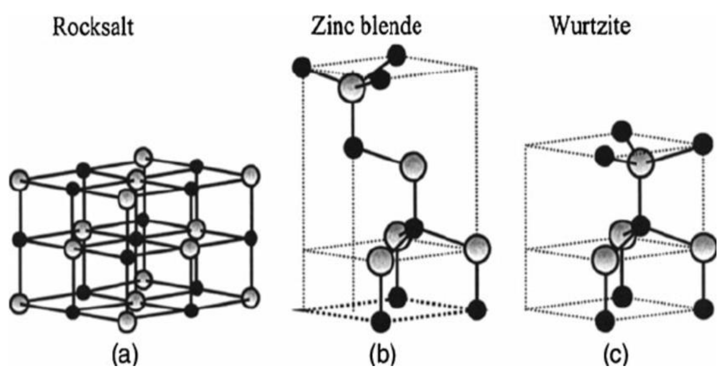

Figure 1.2. Different Crystal Structures of ZnO [8]

ZnO belongs to $p6_3mc$ space group with a lattice parameter, a_0=3.2459 Å, and c_0=5.2069 Å, with a ratio of c/a= √ (8/3) =1.633 as the ideal wurtzite structure [7].

ZnO being a 2-4 compound semiconductor considered as an n-type semiconductor due to structural point defects i.e. vacancies and interstitial defects, mainly due to oxygen vacancies.

- **Electrical Properties**

Possessing a wide band gap of 3.3 eV at room temperature, allows ZnO to have high breakdown voltage, resistance to a high electric field, low electronic noise and high-temperature operation making it suitable for a variety of electrical equipment.

❖ Mechanical Properties

The hardness of ~5 mohs makes ZnO a soft material, Its elastic constant is also small as compared to other material of the same group, high heat capacity, high melting point, high radiation hardness [9, 10] and low thermal expansion are some unique characteristics of ZnO.

❖ Magnetic Properties

Various researchers claimed that magnetic property can be achieved in ZnO by doping at room temperature but preserving it is still a challenge. Though may research are done, the reason behind the origin of ferromagnetism is not clear.

❖ Optoelectronic Properties

Large exciton binding energy of around ~60 meV at room temperature is due to excitonic recombination. Making it a promising material for optical devices. ZnO shows color Emission which can be altered by doping of ZnO or changing the particle size.

❖ Physical properties

Table 1. Physical Properties of ZnO [11-14]

Property	Value
Molecular Mass	81.4084 g/mol
Color	Amorphous White
Density	5.606 g/cm^3

Boiling Point	2360 ^{o}C
Melting Point	1975 ^{o}C
Refractive Index	2.0041
Relative Dielectric Constant	8.66
Intrinsic Carrier Concentration	$<10^{6}$ /cc
Electron Effective mass	0.24
Hole effective Mass	0.59
Hole mobility (room temp)	5-50 cm^{2}/V-s

❖ Doping of ZnO:

Changing the property of a material can also be done by intentional mixing of some impurity called doping or by creating defects in the crystal structure of a material. Though the property can be changed by altering the morphology of material, morphology engineering is limited due to a limited number of processing or synthesis methods, and some morphologies have limitations on their application in technology. Thus doping provides a solution to the question of how to change the property of a material by retaining the same morphology. Doping enhances the optical and electrical properties of ZnO. Various dopants have been studied in the past for ZnO such as, Al^{3+}, Ni^{2+}, Cu^{2+}, N^{3-}, Ga^{3+}, Co^{2+}, Ag^{1+}, F^{1-}, In^{3+}, Fe^{3+}, Fe^{2+}, Sb^{5+}, Sn^{4+}, Mn^{2+},etc [15, 16] . These dopants have their own merit and demerits depending on its ionic radii and electronegativity. It can impart a totally new property in ZnO structure or can enhance the already present property of ZnO which can increase the scope of use of ZnO in new technologies.

4. Application of ZnO

Variety of nanostructures, flexibility of synthesis techniques and growth parameters, and dynamic properties of ZnO material being biocompatible has lead revolution in the field of nanotechnology, researchers in the past have done many novels works by using their knowledge and innovated many devices in many fields either it is biomedical, electrical, optical, mechanical, etc. as can be seen in Figure 3.

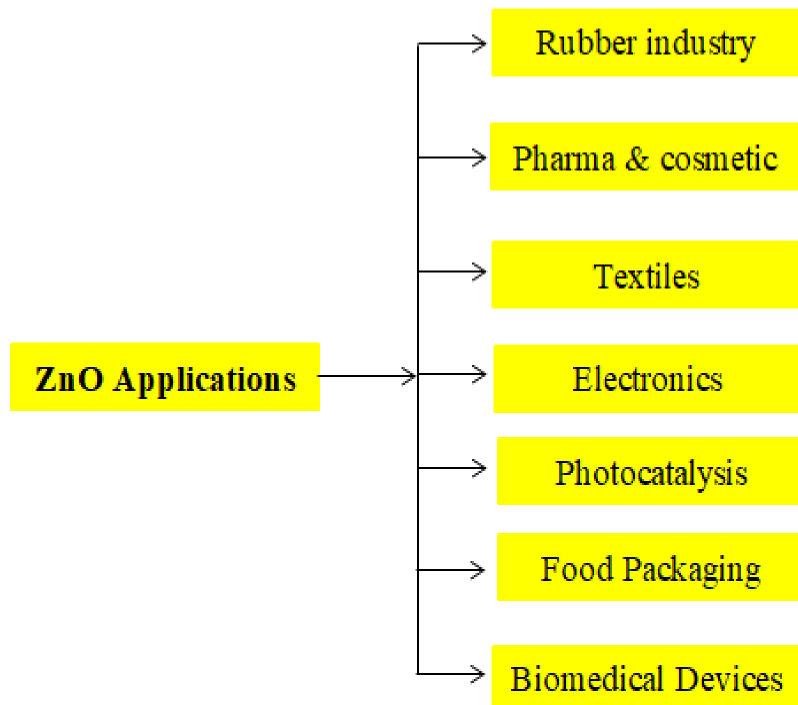

Figure 1.3. Application of Nano ZnO in different fields.

❖ **Rubber Industries**

ZnO is used as a thermally conductive filler which helps in improving the thermal conductivity of silicone rubber while retaining its high electrical resistivity. It is also used as a cross-linking agent in elastomers which generally depends on the morphology of ZnO. It speeds up the process of rubber vulcanization [17].

❖ Pharma and Cosmetic

ZnO is used in various medicines due to its antibacterial, drying and disinfecting properties [18]. ZnO has a property which helps in accelerating wound healing, this property is used in dermatological medicines and cosmetics. ZnO absorbs UV radiations produced by the sun so it is used in sunscreen creams to restrict UV radiation to penetrate in the skin.

❖ Textiles

Anti-bacterial and anti-microbial properties of ZnO makes it a prominent material to be used in textile industries, used as a resistor to textile manufactured products from bacteria and decreases its degradation rate, it also inhibits self-cleaning feature to the manufactured cloth [19].

❖ Electronics

Wide and tunable energy band gap of ZnO and high exciton binding energy at room temperature of ZnO enables it to be used in the electronics industry such as LEDs, Sensors, Solar cells, etc. Its photoluminescent property is used in Field Emission Displays, like T.V.

❖ **Photocatalysis**

ZnO is used as a catalyst for Oxidation and Reduction reaction, to be occurred at its surface by the generation of electron-hole pair produced due to intensity of light, playing the role of photocatalyst it oxidizes the organic pollutant by means of the photogenerated hole [18].

❖ **Food Packaging**

High thermal stability, an anti-bacterial and anti-microbial property of ZnO enables it to be used as a food packaging product. It is non-hazardous, non-toxic, and biologically safe so it can be used for protection of food for a long duration. It is also recognized safe by the US Food and Drug Administration Center [20].

❖ **Biomedical Devices**

High Electron transfer rate, increased Sensitivity and high Iso-electric point (IEP) of about 9.5 and ability to dissolve very slowly at biological pH values [18], anti-bacterial property and UV light activity gained the attraction of researchers for using ZnO as Biosensor material and also using it for cell imaging and drug delivery.

5. Thesis Objective

The objectives of this research work are as follows:

- Synthesis of ZnO and Mn:ZnO with the economically feasible and simple wet chemical method.
- To study the doping effect of Manganese (Mn) in ZnO Structure synthesized via wet chemical approach on Glass substrate.

- To study the effect of Mn doped ZnO on Physico-Chemical properties and thermistor device performance.

6. Thesis Outline

This research work has been systematically divided into seven chapters to give detailed information of the research conducted, from the introduction of ZnO to its Applications and results and discussion of this study.

The chapters content are as follows:

Chapter 1, “Introduction” gives an overview of nanotechnology and nanomaterial and introducing ZnO as a novel material to study, having richness in its properties and making it suitable for a variety of application.

Chapter 2, “Literature Review” deals with different synthesis/growth techniques used for Mn doped ZnO synthesis and comparing them with the simple and economically feasible method of synthesis used in this research work.

Chapter 3, “Characterization Techniques” contains details about different characterization tools used for the study of nanomaterial and presents their working setup and working principle behind the tool to analyze the material.

Chapter 4, “Experimental Method and Materials” emphasize on steps involved in the process of synthesis of Mn doped ZnO and Undoped ZnO and also gives details about the chemistry behind the growth of such nanostructure.

Chapter 5, “Result and discussion” deals with the study of Mn doped ZnO while comparing it to pure ZnO with the help of various Characterization techniques.

Chapter 6, “Temperature sensor” in this chapter the tuned properties of Mn doped ZnO as studied in the earlier chapters, is applied on temperature sensing applications to see how it work as a temperature sensor.

Chapter 7, “Summary and Conclusions and Future Scope” summing up all the results of this thesis an overall conclusion is derived while outlining the future work to be done for further study.

CHAPTER 2

LITERATURE SURVEY

As discussed in the above chapter ZnO is rich in nanostructures and these nanostructures play a crucial role in determining the property of the material, as these properties are very crucial to determine its uses in multifunctional applications[21]. So it is very important to know the nanostructure of the material for determining its property. In the past, researchers have found that this nanostructure can be easily engineered by changing the method of synthesis of material and synthesis conditions, so many techniques are developed in the past to prepare ZnO nanostructures, such as Sol-Gel method, Co-precipitation method, Hydrothermal process, Vapour deposition, Micro emulsion and mechanochemical process [22]. These methods are complicated as it has many synthesis parameters like high temperature, high pressure and lengthy reaction time. These synthesis method needs to be changed with an alternative cost-effective and simple method, in recent days Wet chemical approach has been emerging topic of synthesis of nanostructures having fewer synthesis parameters and provides of ease of substrate selection. This technique allows for the direct implementation of the produced material for multifunctional applications.

- **Selection of Mn as Dopant**

Past studies of Mn Doped ZnO shows that it augments magnetic properties in ZnO nanostructure as observed by Yang et al[19], though the reasons for Magnetic properties of ZnO is still not clear. Some researches state that the magnetic property of this nanostructure is due to Zn doping in MnO. This Magnetic property of Mn doped ZnO can be very useful for spintronics applications. Being a transition metal, with half-filled d subshell. It has variable valence state which can create energy states in ZnO improving its electronic properties. The ionic radii Mn^{+2} is similar to Zn^{+2}. Making it a suitable candidate for doping in ZnO nanostructures.

Table 2. Literature Review of Mn doped ZnO by different synthesis methods with synthesis parameter involved in it.

Methods	**Precursor**	**Synthesis Condition**	**Ref.**
Sol-gel method	$Zn(CH_3COO)_2$, $Mn(CH_3COO)_2$, C_2H_5OH, CH_3OH,$C_6H_{15}NO_3$	Dip coating speed:50 mm/min Calcination:500^{o}C, 1hr	[23]

	$Zn(CH_3COO)_2$, $Mn(CH_3COO)_2$, 2-Methoxyethanol, Monoethanol	Spin coating:3000rpm, 30sec Heating: 300^{o}C, 5 min for each coating, Annealing 650^{o}C, 2hr	[24]
	$Zn(CH_3COO)_2$, Methanol, Manganese (II) chloride	Solution stirring and then Autoclave heating rate 45^{o}C/hr	[25]
	$Zn(CH_3COO)_2$, Methanol, $MnCl_2$, Ethylene glycol	Stirring solution overnight and drying at 110 ^{o}C,1hr Annealing 500 ^{o}C,2hr	[26]
Mechano chemical Process	$ZnCl_2$, Na_2CO_3, NaCl, $MnCl_2$	Milling 5h, 500rpm Heat treatment 600^{o}C, 1hr Drying for 24hrs	[27]

Precipitation method	$Zn(CH_3COO)_2$, NaOH, Isopropyl alcohol, Manganese acetate, Ammonium hydroxide, Ethanol	Stirring 30 mins & kept for 2 hrs, washed filtered & dried. Calcination 600 ^oC,1hr	[28]
	$Zn(CH_3COO)_2$, $Mn(CH_3COO)_2$, Methanol, KOH	Stirring & heating 375K, 2hr Cooled kept for 2 days, washed, filtered and dried at 400K Annealing 8h, 670-1275K	[29]
	$Zn(CH_3COO)_2$, $Mn(CH_3COO)_2$, NaOH, Ethanol	Solution heating 80^oC, 30 min & 60^oC 2hrs, precipitate washed & filtered	[30]
	$Zn(CH_3COO)_2$, $Mn(CH_3COO)_2$,	Solution heating	[31]

	NaOH, Ethanol, H_2SO_4, o-cresol, m-cresol, p-cresol	75^{o}C, 45 min then stirring at 8.3 pH, water bath 67^{o}C, 2hr, RT cooling 4 hr, centrifuged 20 min 4000rpm, dried overnight 110^{o}C Calcination 650^{o}C, 3.5 hr	
	$Zn(CH_3COO)_2$, $Mn(CH_3COO)_2$, KOH	Stirring 70^{o}C, 2 hrs, washed, filtered, dried several days	[32]
	$Zn(CH_3COO)_2$, $Mn(CH_3COO)_2$, NaOH	Stirring 0.5 hr pH 11, heating 40^{o}C,1.5hr, washed, filtered and dried 250 ^{o}C, 7 Hrs	[33]

By concluding from all these literature, synthesis method shown in the above table for Mn doped ZnO is complicated as it has many synthesis parameters like high temperature, high pressure and lengthy reaction time, etc and properties of nanomaterial depend upon the synthesis process.

So, this thesis focuses on minimizing the synthesis parameter of Mn doped ZnO by the synthesis of material by a wet chemical approach.

CHAPTER 3

CHARACTERIZATION TECHNIQUES

1. X-Ray Diffraction

X-Ray Diffraction (XRD) is a characterization tool to study the crystallographic structure, lattice parameters, strain, orientation of crystals, phase, etc. of material by use of X-rays, as the interatomic distance i.e. d-spacing of all matter is of the same order as of X-ray Wavelength (λ~A). This technique is simple, reliable and non-destructive.

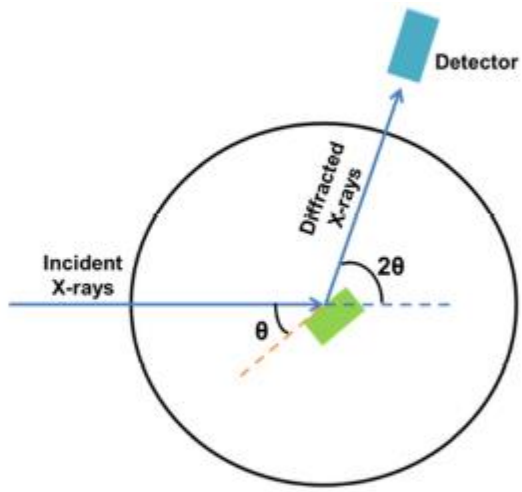

Figure 3.1. Representation of typical X-Ray Diffraction[34]

In this technique, a collimated X-ray beams incidences on the sample material, atoms inside the material diffracts the X-rays beams depending on the d-spacing, according to Braggs law.

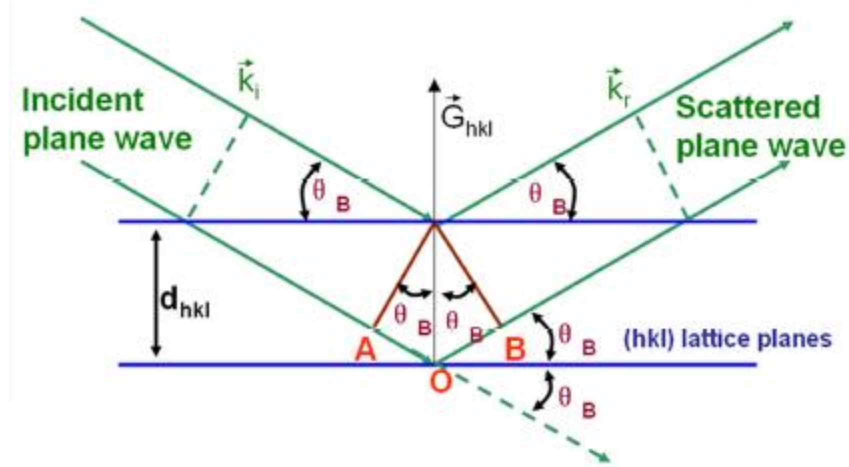

Figure 3.2. Diffraction of incidence X-ray by atom on a crystal plane.[34]

According to Braggs law,

$$\boldsymbol{n\lambda = 2dsin\theta} \tag{1}$$

Where n being an integer, λ is X-ray beam wavelength, d is the interplanar distance of the crystal, θ is the angle made by the atomic plane of the crystal and incidental X-ray beam. An XRD pattern can be plotted between the intensity of resultant of the diffracted peak on the y-axis and angular position of those peaks on the x-axis. Different materials have a different plane orientation with different d-spacing, depicting different XRD patterns, this XRD pattern can be said as a unique signature for a material. By comparing this XRD pattern, with the standard XRD files published by International Centre for Diffraction Data (ICDD), the structure and material composition can be determined, further studying of the XRD pattern lattice parameter, strain, particle size can be determined, etc.

In this research work, XRD measurements are done using Bruker D8 Advance X-Ray Diffractometer, with $Cu\ K_\alpha$ filtered radiation source having wavelength 1.5406 $\AA$, recording the diffraction pattern between 20^o-80^o range of 2θ.

2. Field Emission Scanning Electron Microscopy

FESEM is a characterization tool for morphological analysis of the material, being a non-destructive and non-contact technique for imaging the nanostructures. In this Microscopy technique, a tungsten filament cathode coupled with an electron gun is used to thermionically emit the Electron beam. Tungsten is generally used due to its low Vapour pressure and high melting point among other metals. This electron beam passes through the anode which is positively charged, placed such that it accelerates the Electron beam and focuses it on the material in a raster pattern with the help of condenser lens placed just above the material, the Electron beam then collides with the material and emits back the signal which is detected by the detector. Figure 3.3 shows the schematic arrangement of the FESEM.

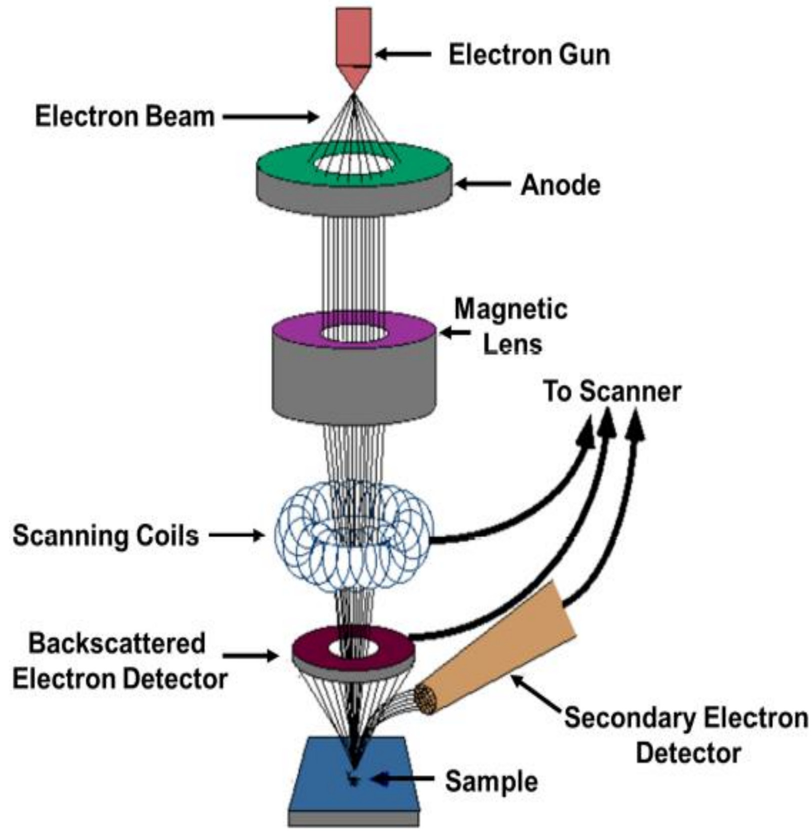

Figure 3.3. Schematic arrangement of FESEM[35]

When an electron interacts with the material it emits Secondary electrons (SE), Backscattered Electron(BSE), Auger Electrons, X-rays, etc.as shown in figure 3.4. But in FESEM, signals of Secondary Electron (SE) and Backscattered Electron (BSE) are detected by the detector to generate the images of nanostructure of material.

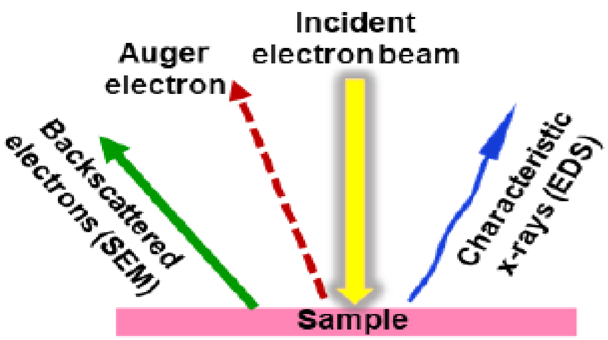

Figure 3.4. Interaction of electron with the material.[36]

a) Secondary Electron:

They are generated due to the inelastic collision of an incident electron with the atom of the surface material, depth of which can be less than 100nm to 5 µm, this electron has low energy less than 50 eV.

b) Backscattered Electron:

They are generated due to the elastic collision of the incident electron with the atom of the material in the bulk, depth of the penetration of incident electron beam depends on its energy, atomic density, and atomic number, this electron beam changes its path after the interaction, it has high energy more than 50 eV.

In this research work, FESEM is done by JEOL JSM-7610F PLUS.

3. UV Visible Spectroscopy

UV-Vis spectroscopy is a tool to analyze the electronic transition of the material. When visible light is incident on the material, the light can interact with the material causing reflection, absorbance, scattering, transmittance and phosphorescence or fluorescence. This light, when absorbed by the material called photon absorption, increases the energy of an electron thus increasing the total potential energy of the molecule of a material which is the sum of their electronic, vibrational and rotational energies.

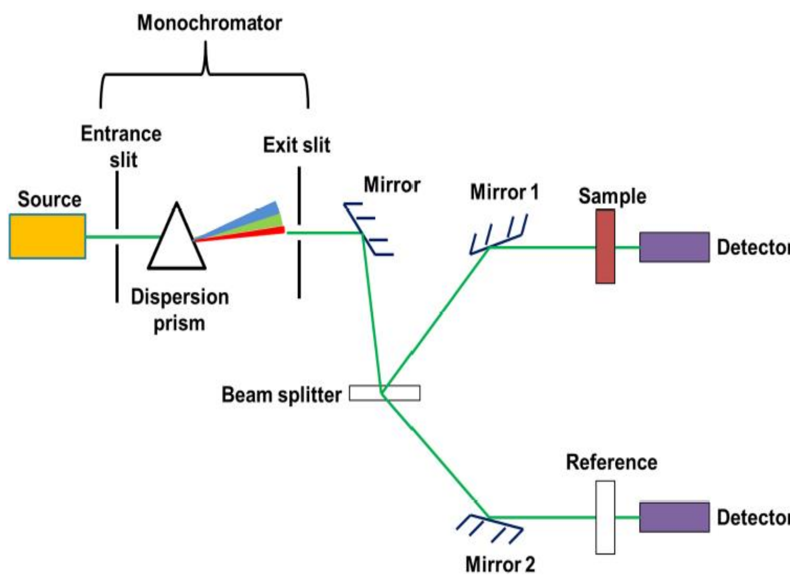

Figure 3.5. Experimental setup of UV Vis spectroscopy[34]

The energy required for the electronic transition of an electron from its lower energy state to higher energy state should be equal to the wavelength of light absorbed. In this spectroscopy, technique light is incident on the material, which is partly absorbed and partly transmitted by the material and therefore a difference in the intensity of incident radiation (I_o) and transmitted radiation (I) occurs due to absorption of the light by the material. Absorbance can be calculated by the following equation 2,

$$\mathbf{A = -log\,(T) = -\,log\,(I/Io)} \qquad \textbf{(2)}$$

Where A = absorbance by the material which is dimensionless, T = transmittance by the material, I=intensity of incident light and I_o=intensity of transmitted light.

4. Photoluminescence Spectroscopy

Photoluminescence spectroscopy is a non-destructive technique to investigate the optoelectronic property of the material. The study of Photoluminescence spectra determines the defect structure, impurity content and energy band levels, etc. of the material. In this spectroscopic tool, the material electrons are excited from valence band to conduction band by providing the photon energy greater than the band gap of the material using laser as a primary source, the excited electron can't stay at the higher energy level for a long time so it tries to return to the lowest energy state i.e. the top level of valence band. And while returning back from the excited state to the top of the valence band it emits energy, in the form of light of different wavelength. However the emitted energy may be less than the photon energy or the energy which is absorbed by the electron for excitation, this energy loss is due to phonons (vibrations) of the lattice. So the PL of a material is largely dependent on its temperature which causes a vibration of the atom on its lattice resulting in its fluctuation of the lattice. A PL spectra is a graph between the emitted light wavelength on the x-axis and resultant emission intensity on the y-axis. Figure 3.6 shows the schematic diagram of PL spectroscopy, which has a laser source for generation of light which is passed through a excitation slit to fall on the material which is placed making an angle

45^o with the monochromatic light, after the light falls on the material it excites the material an emits light of different wavelength in all directions depending on defect state and band gap of the material. A portion of this emitted light is passed through an emission slit and then filtered using a monochromator. As the signal also contains, the signal of low intensity a photomultiplier tube (PMT) is used to detect those low-intensity light. To get emission spectra of emitted light, the particular wavelength is scanned using a monochromator and intensity is recorded by the detector.

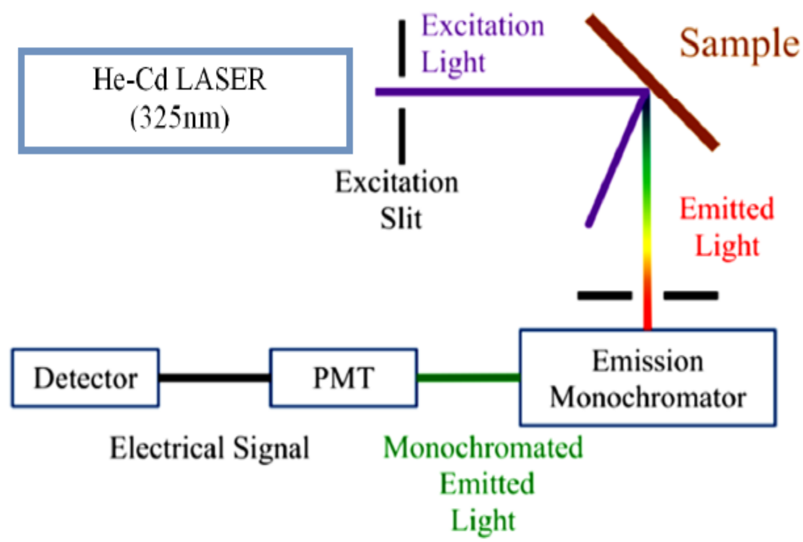

Figure 3.6. Representation of PL spectroscopy[34]

5. Raman Spectroscopy

This Spectroscopic technique is used to identify the molecule or impurity in a material by observing Rotational, vibrational and other phonon modes in a system. It is a non-destructive spectroscopic technique, where Raman scattering (inelastic scattering) of light by the sample is used to study the sample contaminants, functional groups, etc.

Monochromatic light is incident on the sample which interacts with the molecule attached to it, this sample will scatter the light back while part of its energy is consumed in lattice vibration of the functional group or molecule attached, so the scattered light will have energy less than the energy incident by light. This shift in energy or frequency is called Raman shift, if the scattered frequency is less than incident frequency it is said as antistoke, and if the scattered frequency is more than incidental frequency it is said as stokes.

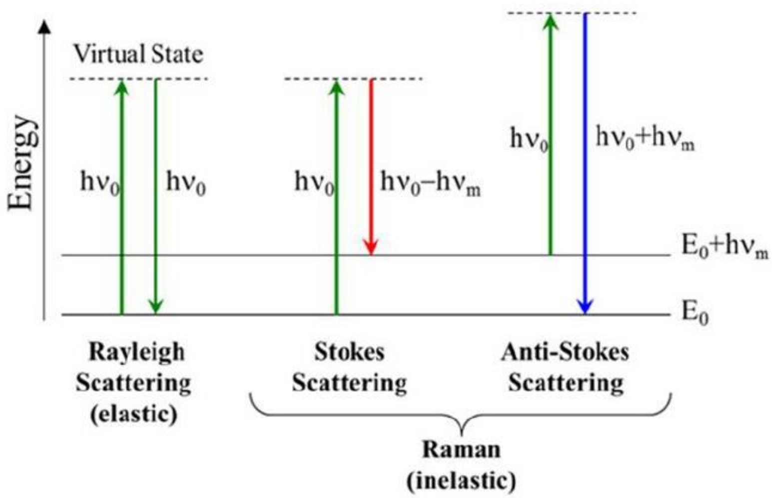

Figure 3.7. Types of Scattering of light by the material. [37]

The shift of wavelength is due to vibrational modes of the molecule. these bands are specific for a specific molecule so we can identify the band shift if a particular material by comparing with it.

In this research work, Raman scattering is done using Labram-HR 800 spectrometer at the excitation wavelength (512 nm).

CHAPTER 4

EXPERIMENTAL METHOD AND MATERIALS

1. Substrate

In an efficient device for any application, selection of material, cost, the property of the material used, etc. are some of the key points to be kept in mind for device fabrication. So each and every material used in device fabrication is to be dealt with proper care and study. As this thing can hamper the working of the device if not choose wisely because the physics of a device depends on its property. So the selection of substrate also plays an important role in the efficient working of the device. Depending on the working of device substrate can be chosen, for conduction of charge from the substrate conductive substrate is used like FTO, ITO, etc. while in case if there is no need of conduction of charge from the substrate, non-conductive substrates can be used as glass, etc. The substrate also plays an important role in the adhesion and growth of the nanomaterial. In the case of nanomaterial, higher deposition or higher thickness can be obtained if the synthesized material and substrate lattice match.

- **Substrate Selection**

In this research work, to study the effect of Mn doping in ZnO lattice Glass substrate is used, this glass-based device is used for characterization of material and to know the property of material synthesized. While for application of Mn doped ZnO in multifunctional devices conductive substrate is used.

- **Glass substrate**

  Borosilicate Glass is chosen due to its transparency in the spectral range of our interest i.e. from UV to near infrared spectrum range, excellent flatness, and rigidity, it has a very low coefficient of thermal expansion, resistant to corrosion, and chemically inert[38].

- **Substrate Cleaning**

Cleaning of substrate is an important step before the use of substrate for deposition because substrate may contain residues, dirt, organic or inorganic contaminant. This impurity if not cleaned prior to use of the substrate it may have an ill effect on the device fabricated. So before using the substrate we have cleaned it to remove those contaminants. Generally, ultrasonic cleaning is done to clean the substrates, in this cleaning system ultrasonic sound is used to produce ultrasonic waves with high frequency, this process creates bubbles on the substrate surface, these bubbles try to burst, to exert a force on the substrate surface. Due to which contaminant adhered on the substrate surface is removed

[39]. Any type of solvent can be used to remove the contaminant depending on the contaminant. Substrates are immersed in these solvents and ultrasonicated for a variable time. The surface of the substrate should always be kept free from touching the wall of the beaker so that proper bubble formation can occur at the substrate surface. First, we have cleaned the substrates by gently scrubbing with the help of cotton to remove residues then we have cleaned the substrate with ultrasonic cleaning method for 15 minutes by using 3 different solvents, Double Distilled water for removing of dirt and detergents present over the surface. Acetone solvent is used to remove grease, while Ethanol is used to remove organic and inorganic contaminants present over the substrate surface. Figure 4.1 shows the procedure of cleaning the substrates.

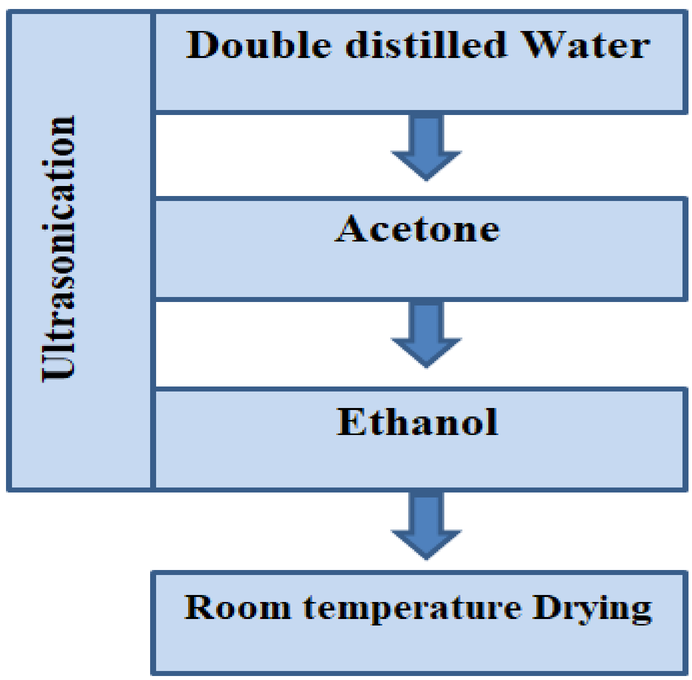

Figure 4.1. Procedure for substrate cleaning.

2. Wet Chemical Synthesis

The wet chemical synthesis approach is the method we have used in the synthesis of material. This method is also referred to as chemical bath deposition method [40, 41]. This method is economically feasible and reliable which needs less sophisticated instruments, it only requires a container filled with depositing material solution and some holding equipment with a temperature controlled oil bath for maintaining reaction temperature. This method is also suitable for perfectly oriented growth of material with single step deposition directly on the substrate surface without the need for seed layer deposition. This method produces material with uniform and adherent coating with excellent reproducibility.

In this method, the thickness can be controlled by controlling the parameters like pH of the solution, time, temperature and the concentration of chemical used in material synthesis. These parameters can be easily changed to get the desired thickness. However, the growth of the thin film depends on the chemical reaction of the precursor and complexing agent added in the solution [40]. In this method, first, the precursor material is dissolved in a solvent to make a solution in a container and stirred till it makes a homogeneous solution then a complexing agent is added, and the desired pH is maintained of the solution. After which the clean substrates are immersed vertically into the solution and the container is now kept into the oil bath maintained at the desired temperature for a desirable time depending upon the need of thickness of the material.

In our research, we have chosen Zinc Acetate dehydrated [$Zn(CH_3COO)_2.2H_2O$] as precursor material for ZnO deposition while for Mn doped ZnO synthesis, Zinc Acetate dehydrated [$Zn(CH_3COO)_2.2H_2O$] and Manganese(II) Acetate [$Mn(CH_3COO)_2$] is used as the precursor material which is dissolved in Double Distilled water to make 100 mM solution, Ammonia solution (NH_4OH) is used as a complexing agent, which is added dropwise to the solution kept for stirring, maintaining the solution at around 11 pH. Simultaneously Glass and ITO substrate was dipped in the solution vertically and this solution is kept in an oil bath maintained at 100 ^oC for 1 hour. Finally, the deposited substrates were removed from the solution and washed thoroughly with double distilled water to wash the precipitate formed over the coating and then these deposited substrates were air dried. Figure 4.2 shows the procedure of material synthesis.

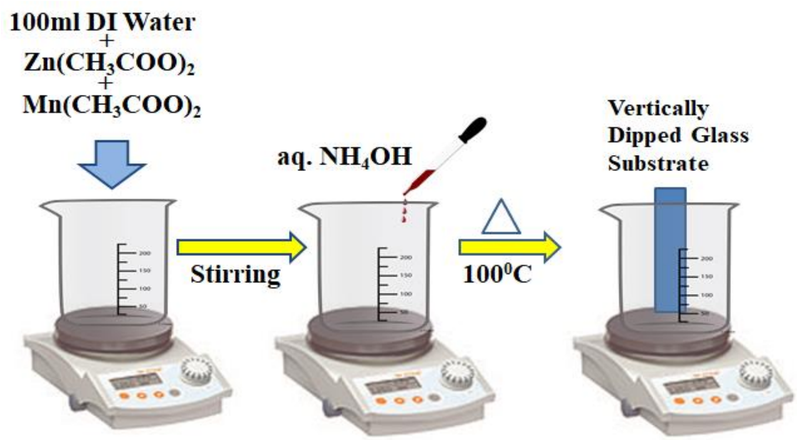

Figure 4.2. Synthesis process involved in the material synthesis.

3. Chemistry Behind Material Deposition in CBD

The growth of the material over the substrate is governed by the chemical reaction involved in the solution. When the precursor material is dissolved in water it forms metal ion and complex ion species. When a complexing agent is added to the solution, it reacts with the metal ion forming metal hydroxide while the precursor metal complex reacts with the complexing agent complex ion forming precipitate. While adding the complexing agent it is necessary to keep in mind that excess mixing of complexing agent will lead to excess formation of a precipitate, so the solubility product value should be kept less than ionic product value. The metal hydroxide thus formed can be used for deposition of metal oxide on the substrate by a thermal decomposition reaction.

- **Plausible ZnO growth chemistry[42].**

Zinc Acetate [$Zn(CH_3COO)_2$] dissociates into Zn^{2+} (Zinc ions) and CH_3COO^- acetate ions when dissolved in double distilled water as can be seen in reaction 3. When ammonia solution is added into the solution, it also dissociates into NH_4^+ ions (ammonium ion) and OH^- ions (hydroxide ions) as shown in reaction 4.

$$Zn(CH_3COO)_2 + H_2O \longrightarrow Zn^{2+} + (CH_3COO)^- \qquad (3)$$

$$NH_4OH \longrightarrow NH_4^+ + OH^- \qquad (4)$$

Zinc ions (Zn^{2+}) then reacts with the hydroxide ion (OH^-) and will form Zinc hydroxide [$Zn(OH)_2$] and the acetate ion [CH_3COO^-] will react with ammonium ion [NH_4^+] forming ammonium acetate [NH_4CH_3COO or $C_2H_7NO_2$] as shown in reaction 5 & 6 respectively.

$$Zn^{2+} + 2OH^- \longrightarrow Zn(OH)_2 \qquad (5)$$

$$NH_4^+ + (CH3COO)^- \longrightarrow NH_4CH_3COO \qquad (6)$$

When these reactions are completed substrates are dipped in the solution and kept in an oil bath maintained at a certain temperature. Hence a thermal decomposition reaction will take place and Zinc hydroxide [$Zn(OH)_2$] will decompose into ZnO formation on to the substrate surface as shown in reaction 7.

$$Zn(OH)_2 \longrightarrow \mathbf{ZnO} + H_2O \qquad (7)$$

ZnO nanostructure will finally be deposited on the substrate.

CHAPTER 5

RESULTS AND DISCUSSION

(1) Morphological properties

Scanning Electron Microscopy

Figure 5.1 shows as obtained SEM images at 50 kX and scale 100 nm, of the Mn doped and undoped ZnO on Glass substrates. The images show that the structure grown on the glass substrate is having nanorods like structure having a hexagonal shape and the diameter of the rods is the same throughout the length. On analysis of this Structures the average diameter of the rods are measured, the measured average diameter of undoped ZnO is found to be around 300 nm, while average diameter of Mn doped ZnO is found to be ~160 nm, ~250 nm, ~180 nm, ~130 nm for 5%, 7.5%, 10% and 12.5% Mn doping, respectively. This shows that the measured average diameter of the doped nanorods is considerably reduced to half when compared to undoped nanorods. Also, the length of rods became shorter with Mn doping. This is due to the reason that the atomic size of Mn (117 pm) is lower than Zn (125 pm). This data is also well matched with XRD data.

While comparing images in figure 5.2 at 10000X and scale 1µm of Mn doped and undoped ZnO structures, we found that the density of nanorods over the substrate surface is increasing with Mn doping concentration.

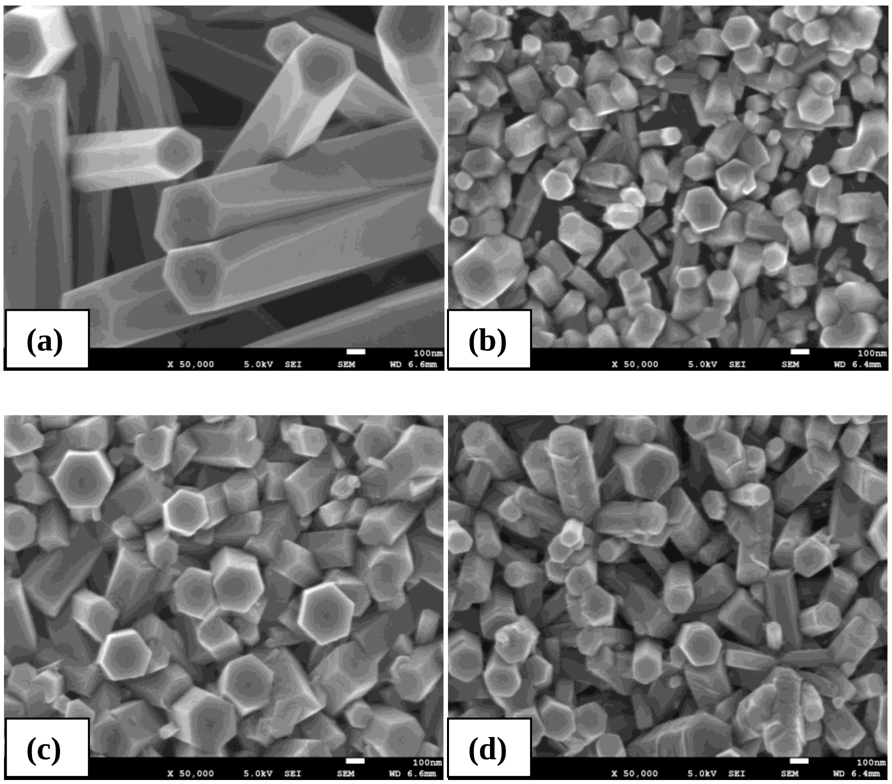

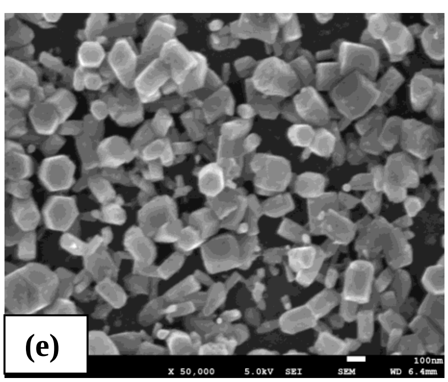

Figure 5.1. FESEM images at 50 kX and scale 100nm of (a) undoped ZnO, (b)5%Mn:ZnO, (c)7.5%Mn:ZnO, (d)10%Mn:ZnO, (e)12.5%Mn:ZnO.

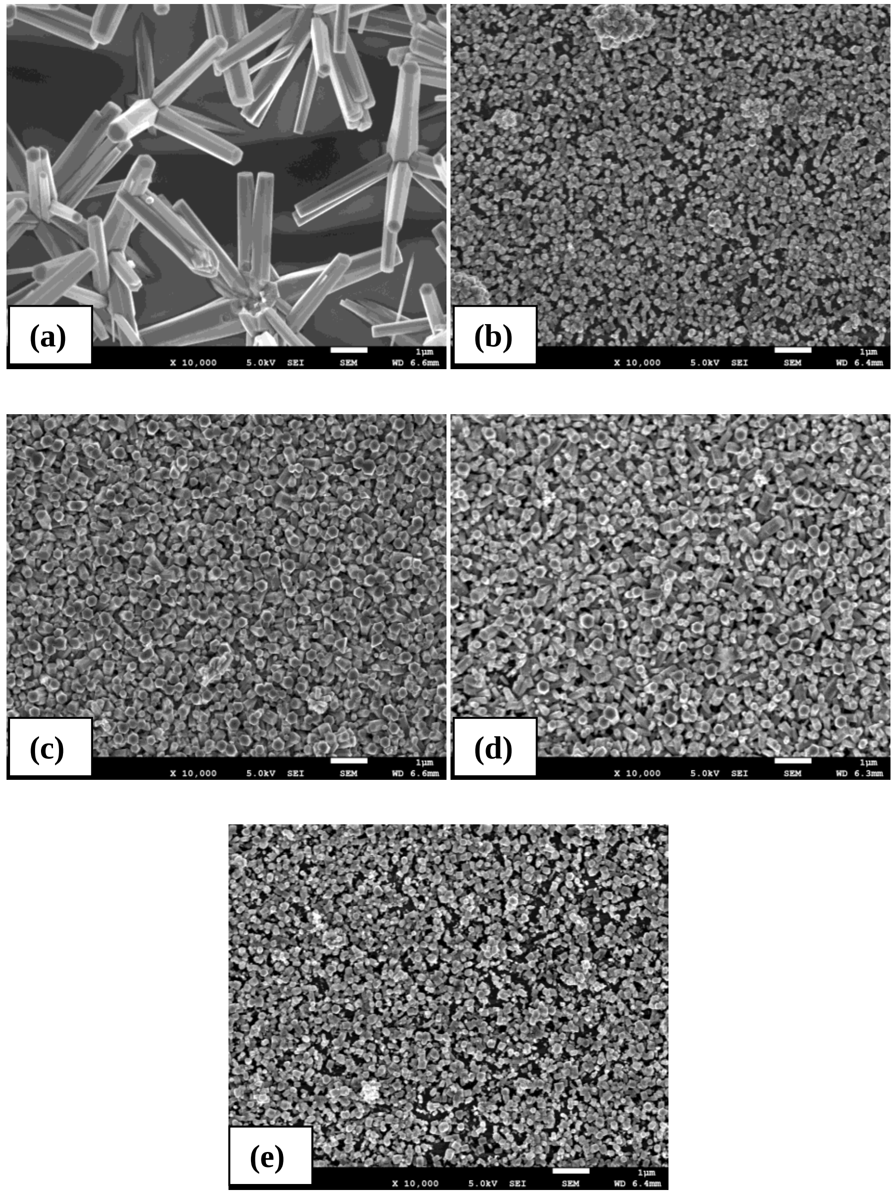

Figure 5.2. FESEM images at 10KX and scale 1µm of (a) undoped ZnO (b) 5%Mn: ZnO (c) 7.5%Mn: ZnO (d) 10%Mn: ZnO (e) 12.5%Mn: ZnO.

(2) Structural Properties

X-Ray Diffraction

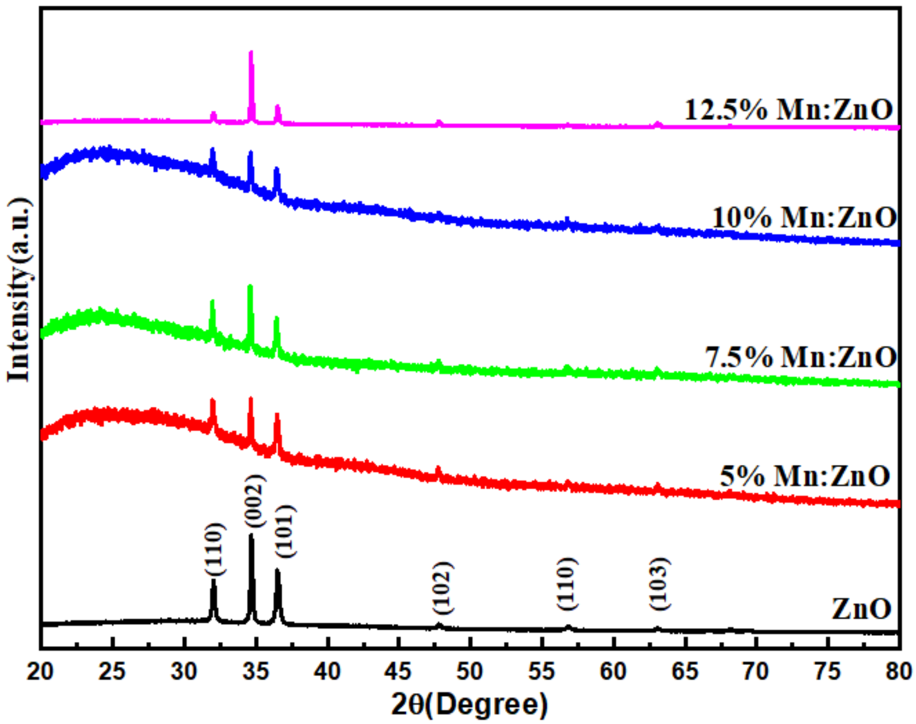

Figure 5.3. XRD pattern of Mn doped and undoped ZnO

Figure 5.3 shows the XRD pattern for Mn doped and undoped ZnO in 20^0 to 80^0 degree diffraction angle range. Study of XRD parameter shows that all the diffraction peaks of Mn doped and undoped ZnO match with ZnO wurtzite phase (JCPDS 79-0205, Space group $P6_{3m}c$). No impurity peaks were found in any of the samples whereas none of the peaks vanished due to Mn doping which means Mn doping does not change the wurtzite phase of ZnO. The diffraction pattern shows that in all samples the intensity of (002) peak is highest, indicating the density of growth is along (002) plane, so we can say that the growth is preferred to be along *c*-axis rather than another axis. It is also seen that with increase in Mn doping, (002) peak shifted toward lower two theta values as shown in figure 5.4(i) which can be stated as the incorporation of higher radii Mn^{+2} ion(0.83Å) in ZnO lattice replacing lower radii Zn^{+2} ion(0.74 Å).

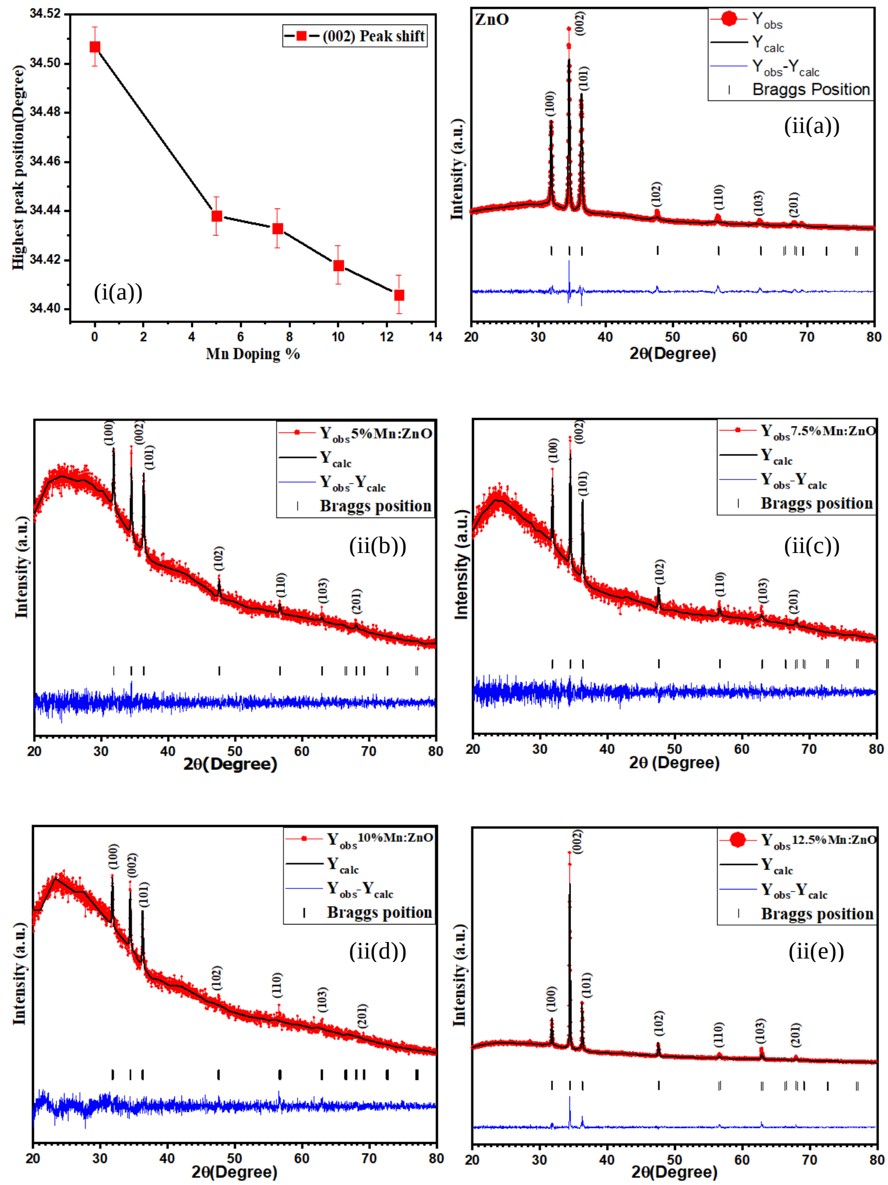

Figure 5.4. (i) Variation of (002) peak with Mn doping (ii) Rietveld Refinement XRD pattern of (a) undoped ZnO (b) 5%Mn: ZnO (c) 7.5%Mn: ZnO (d)10%Mn:ZnO (e) 12.5%Mn: ZnO.

For further structural analysis of all samples like lattice parameter, unit cell volume, bond length, particle size and degree of distortion, Rietveld Refinement is done using FullProf software as shown in figure 5.4(ii). Variation of Lattice parameter with Mn doping is shown in Figure 5.5(a), it can be seen that with Mn concentration *a* and *c* lattice parameter increases. Unit cell volume(V) and Average bond length(L) is calculated using equation 8 & 9, respectively [43].

$$\mathbf{V=0.866a^2c} \tag{8}$$

$$\mathbf{L}= \sqrt{\frac{a^2}{c} + (0.5 - u_p)^2 c^2} \tag{9}$$

$$\mathbf{u_p}= \frac{a^2}{3c^2} + 0.25 \tag{10}$$

Where *a* and *c* are lattice parameters, V is unit cell Volume, L is Bond length, u_p is positional parameter calculated using equation 10 [43], defined as bond length parallel to the *c*-axis.

Variation of unit cell volume (V) and Bond Length (L) with an increase in Mn doping is shown in Figure 5.5(*b*). It can be seen that Volume and Bond Length is Increasing with an increase in Mn concentration. This increase in lattice parameter, unit cell Volume and bond length is also due to the replacement of lower radii Zn^{2+}ion with higher radii Mn^{+2}ion.

The increase in unit cell Volume, lattice parameter, and Bond Length will lead to distortion of ZnO crystal lattice, due to the incorporation of Mn^{+2} ions. The degree of distortion (R) can be calculated using equation 11 [43].

$$R = \frac{2a(\frac{2}{3})^{\frac{1}{2}}}{c} \tag{11}$$

Where, R=1 is Wurtzite structure ideal value and *a*, *c* are lattice parameters. Variation of degree of distortion is shown in figure 5.5(*c*).

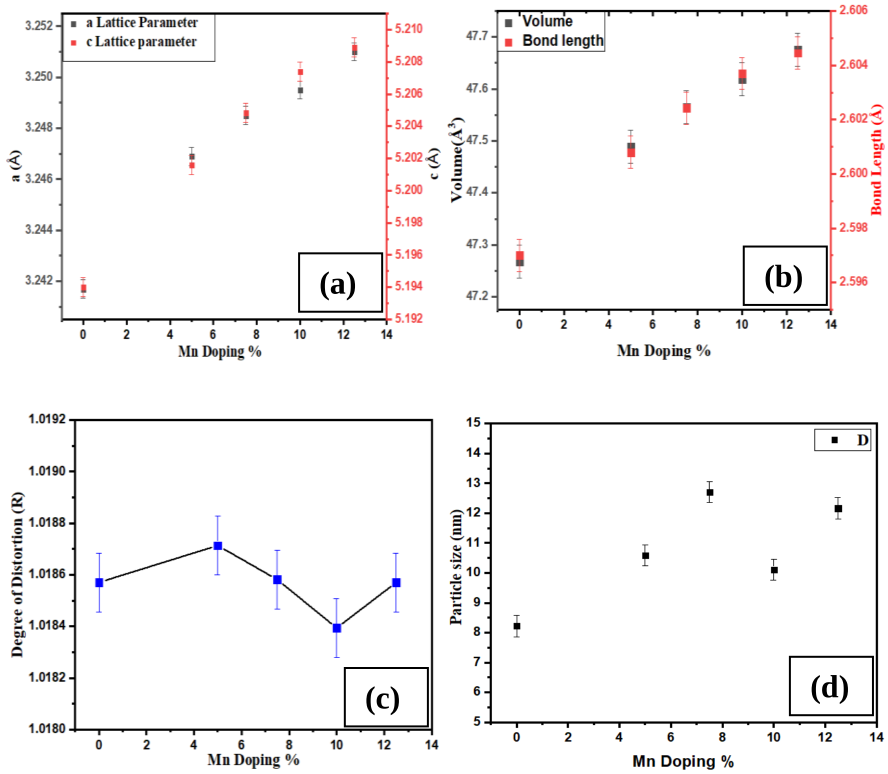

Figure 5.5. (a) Variation of lattice parameter (*a* & *c*), (b) Variation of unit cell volume (V) and Bond Length (L), (*c*) Variation of Degree of Distortion, and (*d*) Variation of Particle size, with Mn doping %.

Particle size (D) of Mn doped and undoped ZnO is calculated using Debye Scherer's Formula given in equation 12 [44].

$$\mathbf{D=\frac{K\lambda}{\beta_{hkl}\cos\theta}} \qquad \mathbf{(12)}$$

where D is Particle size, K is shape factor (0.9), λ is the wavelength of Cu(k_α) radiation, β_{hkl} is FWHM of a selected peak. Variation of Particle Size (D) with Mn doping is shown in the figure5.5(d). It can be seen that the particle size increased when Mn is doped in ZnO lattice and on further addition of Mn particle size almost remain unchanged. This increase is due to the generation of strain in nanostructure produced due to Mn ion replacing Zn ion.

Raman Spectroscopy

Optical phonon modes of ZnO are shown in schematics of figure 5.6. Figure 5.7 shows Raman spectra for Mn doped and undoped ZnO in the range of 70 cm^{-1} to 700 cm^{-1} performed at room temperature via Labram Raman spectrometer.

Group theory analysis of wurtzite ZnO structure, the total number of atoms per unit cell is s = 4, space group P63mc, at the Brillouin zone center (q = 0) shows that phonon dispersion of ZnO has 12 branches as shown in figure 18 consists of polar modes ($A_1$and E_1), two non-polar modes ($2E_2$) and two silent ($2B_1$) Raman modes. Among these, A_1 and E_1 polar modes are divided into 2 active phonon modes (transverse optical (TO) and longitudinal optical (LO)), E_2 is divided into $E_2^{low}$and E_2^{high} active modes and the B_1 branches are Raman inactive modes. This optical phonon mode is represented as equation 13 [45],

$$\Gamma opt = A_1 + E_1 + 2E_2 + 2B_2 \qquad (13)$$

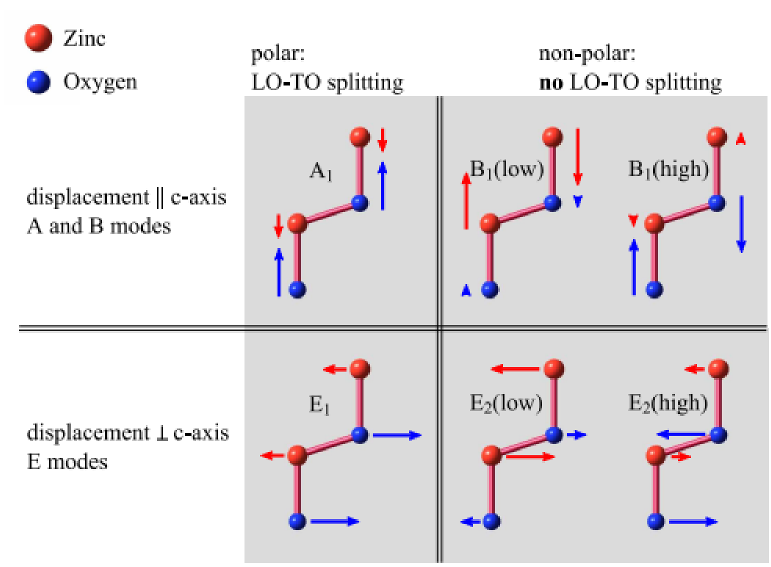

Figure 5.6. Optical phonon modes of ZnO

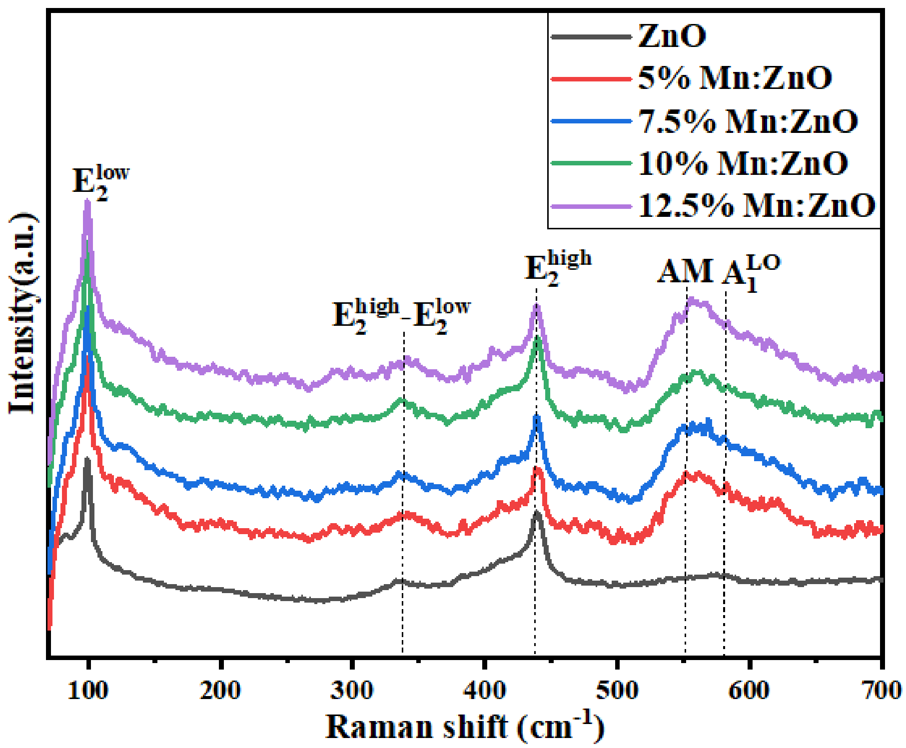

Figure 5.6. Raman Spectra of Mn doped and Undoped ZnO.

On analysis of Raman spectra for Undoped ZnO and Mn doped ZnO, it is seen that one broad peak around 550 cm^{-1} (AM) is seen in all Mn doped ZnO which is not a characteristic peak of ZnO, which can be attributed as Mn impurity vibration related peak also reported by Strelchuk *et al.* [45]. With an increase in Mn doping, the intensity of these peaks increased confirming that it belongs to Mn impurity. All other peaks of Mn doped ZnO match with ZnO characteristic peaks. For all samples, we found E_2^{low} peak at around 99cm^{-1} and E_2^{high} peak at around 440 cm^{-1}. These two peaks are characteristic peaks of ZnO. However the E_2^{high} peak shifted toward lower frequency and the intensity is also decreased with an increase in Mn doping, the shift toward lower wavenumber can be justified by an increase in bond length as seen in XRD results. As reported by

Russo et al [46], $E_2^{\ low}$ mode of ZnO is due to lattice vibration of heavy Zn atom, while $E_2^{\ high}$ mode of ZnO is due to lattice vibration of O atom. So decrease in intensity of peak can be seen as the vacancy of the atom from its lattice position.so decrease $E_2^{\ high}$ can be seen as oxygen deficiency. A peak at around 343 cm^{-1} is reported as (E_2^{high}- E_2^{low}), ascribed as a second-order mode of multiphonon process and A_1(TO). A peak at around 582 cm^{-1} is ascribed as A_1(LO).

(3) Optical Properties

UV-Visible spectroscopy

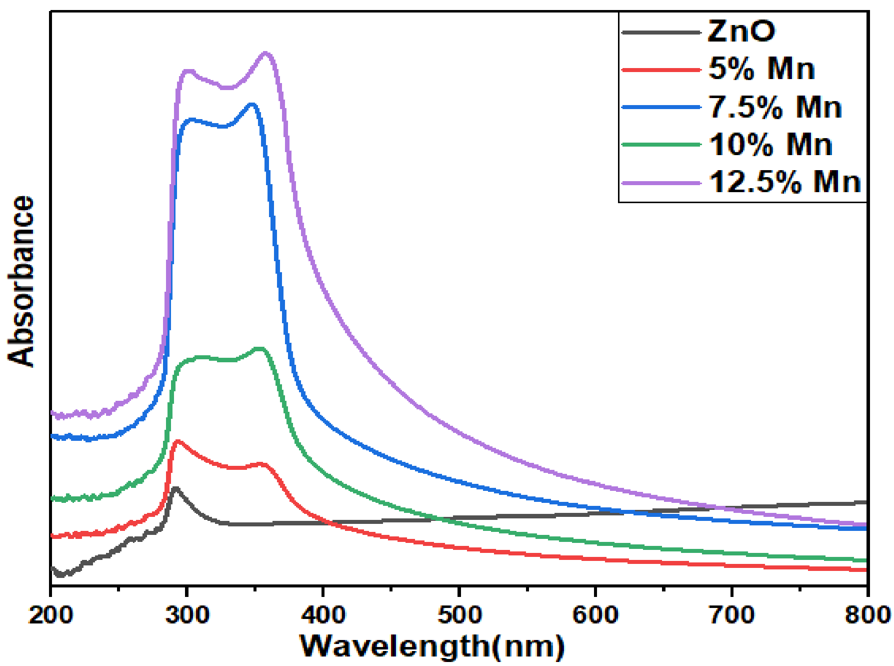

Figure 5.7. Room temperature UV-Visible spectra of Mn doped and undoped ZnO

Figure 5.7 shows UV-Visible absorption spectra of Mn doped and undoped ZnO in the range of 200 to 800 nm performed at room temperature via UV-Visible spectroscopy.

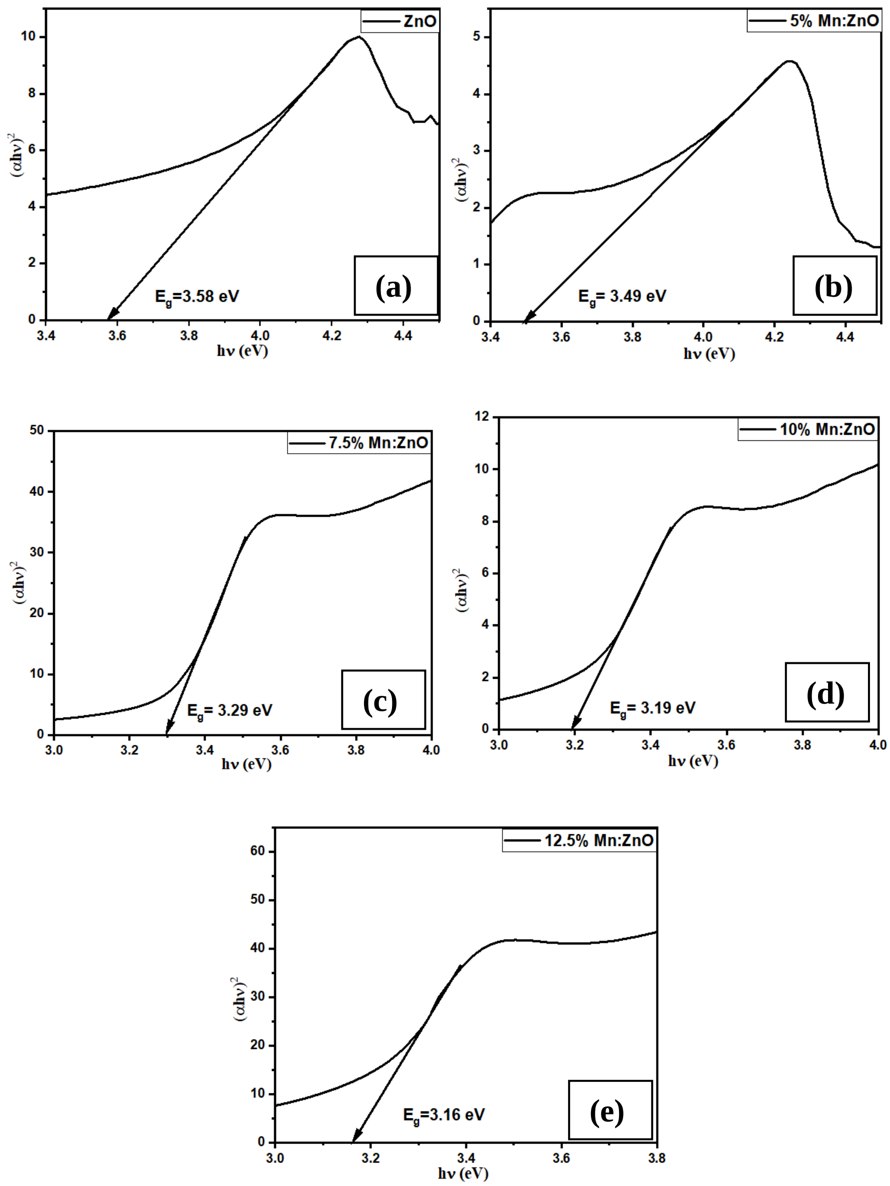

Figure 5.8. Band gap of (*a*) undoped ZnO (*b*) 5%Mn: ZnO (*c*) 7.5%Mn: ZnO (*d*) 10%Mn: ZnO (*e*) 12.5%Mn: ZnO

Figure 5.8 shows the band gap variation of Mn doped and undoped ZnO. Analysis of UV-Visible absorbance spectra shows that with Mn doping the absorption range of the undoped ZnO is increased, showing strong UV absorbance and shifting the curve towards the visible region. The increase in UV absorbance is possibly due to an increase in density of nanostructure over the substrate as found through FESEM images with an increase in Mn concentration.

For calculating the band gap of Mn doped and undoped ZnO, we have used the Tauc Plot method. This method contains a graph, plotted between $(\alpha h\upsilon)^2$ on Y-axis and $h\upsilon$ on X-axis i.e. energy axis, for determination of band gap a vertical line of $(\alpha h\upsilon)^2$ is extrapolated on the energy axis i.e. $h\upsilon$ on X-axis by using Tauc Plot equation 14 [22],

$$\alpha h\upsilon = A(h\upsilon - E_g)^n \qquad (14)$$

Where, α is absorption coefficient, h is Plank's constant, υ is the incident photon intensity, A is the absorbance constant, E_g is band gap of the material and n is a constant having value 2 for indirect and 2.5 for direct band gap semiconductor.

Mn Doping %	**Calculated Band Gap (eV)**
0	3.58
5	3.49
7.5	3.29
10	3.19
12.5	3.16

Table 3. Variation in Bandgap of ZnO with Mn doping

As determined by Tauc Plot method, the Bandgap of undoped ZnO is 3.58 eV and it decreases with increase in Mn concentration as can be seen from Table 3 showing the variation of band gap with Mn concentration. The decrease in the band gap of ZnO with Mn concentration is due to exchange interaction between '*s-p*' electrons of Zn atom and 'd' electrons of Mn atom contributing to *s-d* and *p-d* interaction. This similar observation is also reported by S. Fabbiyol *et al*. [47].

(b) Photoluminescence spectroscopy

The room temperature PL Spectra of Mn doped and undoped ZnO is shown in figure 5.9 which consists of 2 peaks. One being the Near Band Emission at a wavelength around 390 nm, and the other being a broader and wide deep level emission from a range of around 475 nm to around 750 nm in all the samples. However, there seems to be a Blue shift in the NBE and DLE with the increase in Mn doping in ZnO nanostructure. Furthermore, the increase in emission intensity of NBE and decrease in emission intensity of DLE can also be seen from the PL spectra.

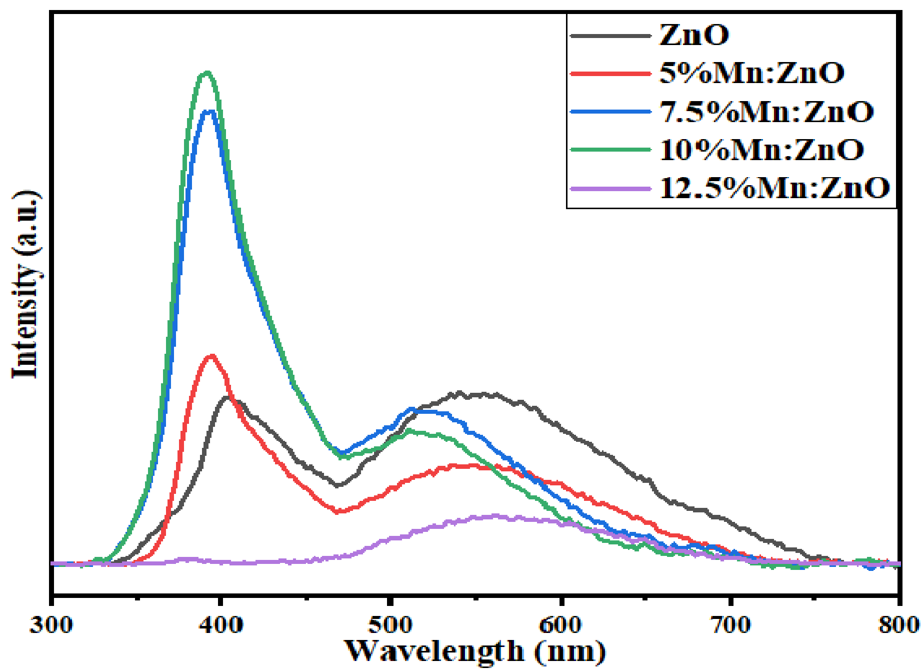

Figure 5.9. PL spectra of Mn doped and Undoped ZnO

The Emission due to Electron-Hole Recombination corresponds to Near Band Emission, occurring due to Exciton pair collision [48]. And the emission due to defects corresponds to Deep Level Emission. There are different defects which are reported in the previous researches like interstitials, vacancies, and antisites of Oxygen and Zinc atom in the lattice structure of ZnO which plays a crucial role in the electronic transition of the electron, creating different electronic states in between valence band and conduction band. This vacancy V_{Zn}, V_O, Zn_i, O_i, Zn_O are reported in the previous reports[49] and a Schematic diagram of energy emission of transition has been derived from these researches as shown in figure 5.10 [50].

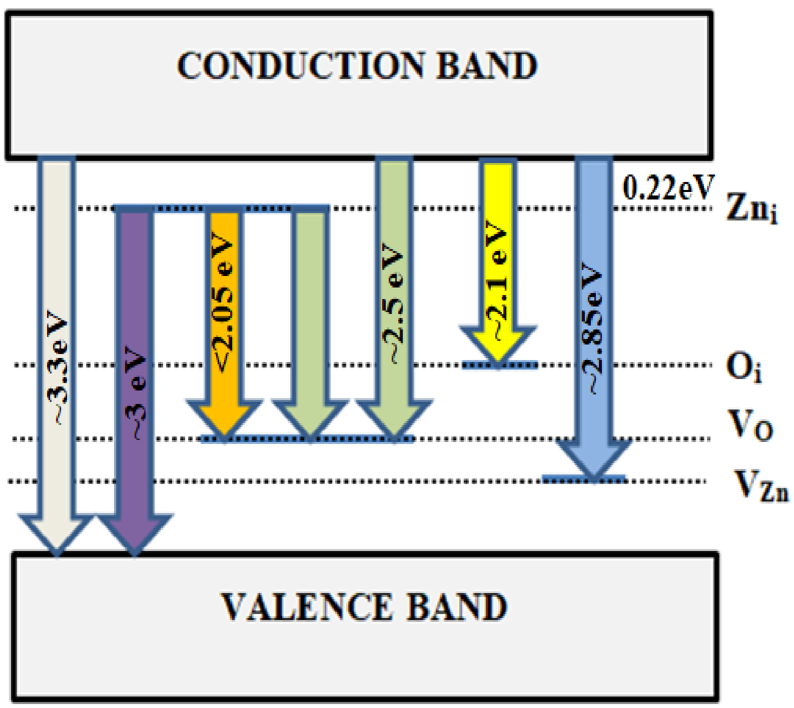

Figure 5.10. Emission of different colors due to different electronic transition [50]

Figure 5.11 shows the Fitted PL spectra of Mn doped and undoped ZnO, this all Spectra are fitted into 6 peaks. For the fitted undoped ZnO sample, the Peak E_1 at 3.08 eV corresponds to free Exciton, Peak E_2 at 2.97 eV corresponds to violet emission occurring due to electron transition from Zn_i to VB, Peak E_3 at 2.41 eV corresponds to blue emission due transition between CB to V_{Zn}, Peak E_4

at 2.19 eV corresponds to green emission occurring due to transition from CB to V_O and Zn_i to V_O, Peak at E_5 at 1.99 eV corresponds to yellow emission occurring due to transition between CB to O_i, and a Peak at E_6 at 1.78 eV corresponds to orange-red transition occurring due to transition between CB to O_i and Zn_i to O_i.

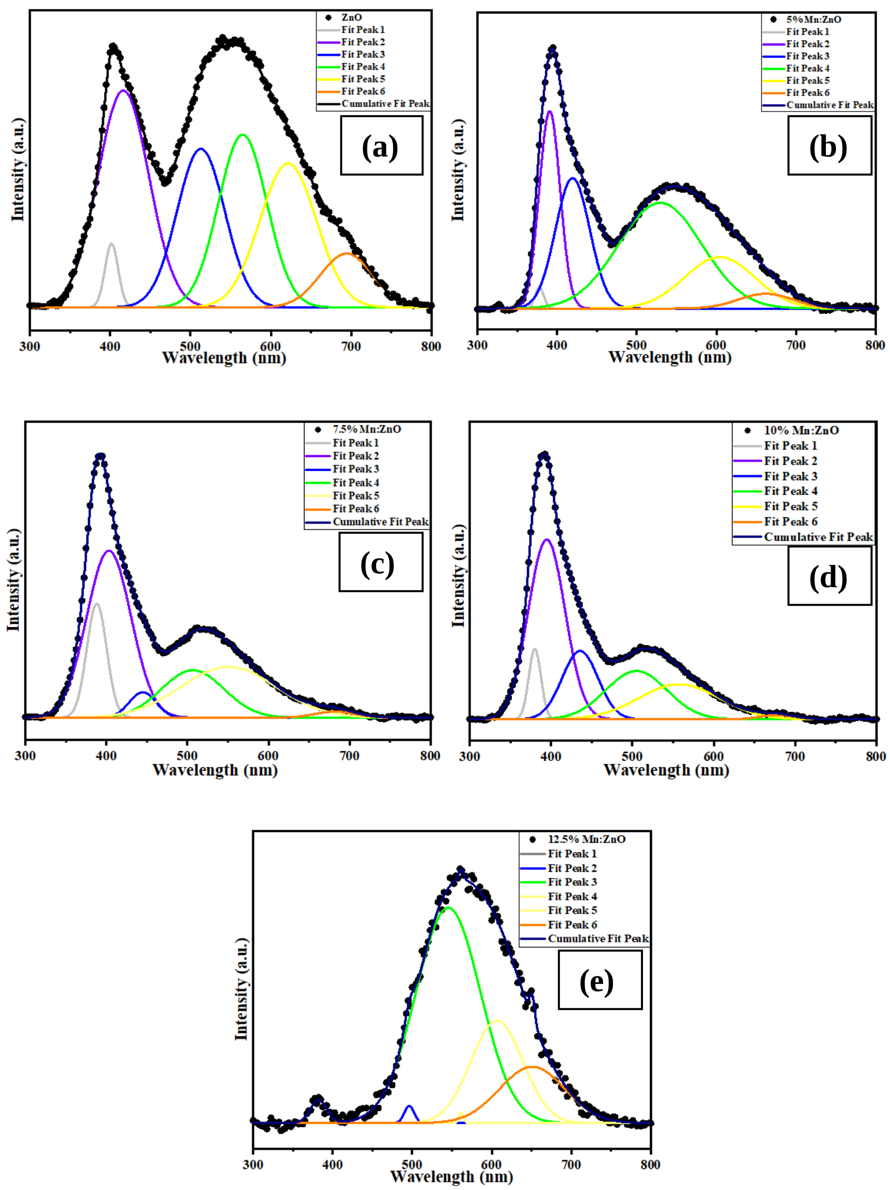

Figure 5.11. Fitted PL spectra of (a) undoped ZnO (b) 5%Mn: ZnO (c) 7.5%Mn: ZnO (d) 10%Mn: ZnO (e) 12.5%Mn: ZnO.

For the fitted Mn doped ZnO sample, the Peak E_1 at 3.28 eV, 3.26 eV, 3.24 eV for 5% Mn, 10% Mn, 12.5% Mn doped ZnO, respectively corresponds to free Exciton, Peak E_2 at 3.17eV, 3.07 eV, 3.14 eV for 5%Mn,7.5% Mn, 10% Mn doped ZnO respectively corresponds to donor level just below the conduction band, the transition from donor level to valence band is the reason for this emission, as also found by Lin *et al.* [51], Peak E_3 at 2.95 eV, 2.79 eV, 2.84 eV for 5%Mn,7.5% Mn, 10% Mn doped ZnO respectively corresponds to blue emission due transition between Zn_i to VB and Peak E_4 at 2.34 eV, 2.44 eV, 2.45 eV, 2.49 eV for 5% Mn, 7.5% Mn, 10% Mn and 12.5% Mn doped ZnO respectively also corresponds to blue emission occurring due to transition from CB to V_{Zn}, Peak at E_5 at 2.05 eV, 2.25 eV, 2.22 eV for 5% Mn,7.5% Mn, 10% Mn, respectively and 3 peaks for 12.5% Mn doped ZnO at 2.27eV, 2.20 eV, 2.04 eV corresponds to green emission occurring due to transition between CB to V_O and Zn_i to V_O, and a Peak at E_6 at 1.87 eV, 1.81 eV, 1.82 eV, 1.90 eV for 5%Mn,7.5% Mn, 10% Mn and 12.5%Mn doped ZnO respectively corresponds to yellow transition occurring due to transition between CB to O_i.

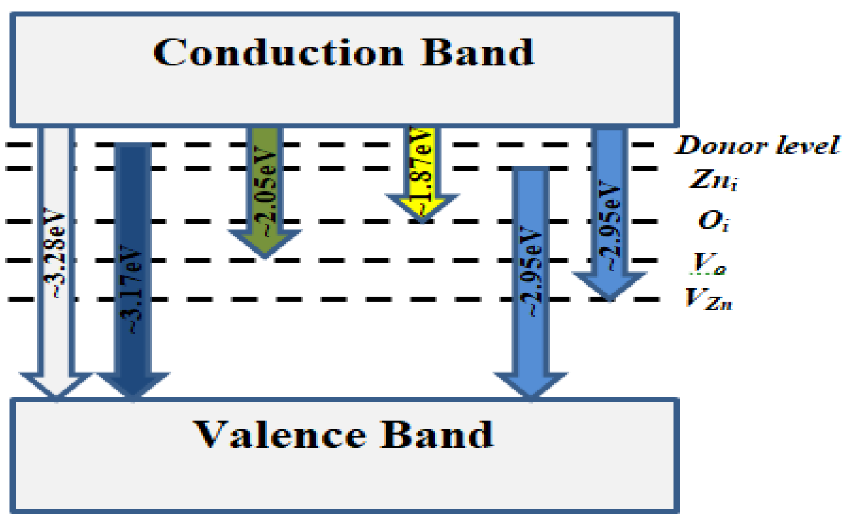

Figure 5.13. Color emission due to defect-related electronic transition of Mn doped ZnO.

Figure 5.13 shows the color emission due to electron transition from different defect related energy level generated due to Mn doping in ZnO crystal structure, as obtained from the above-studied PL spectra of Mn Doped ZnO sample.

CHAPTER 6

Temperature Sensor

1. Introduction

Since every chemical, biological, mechanical, electronic, and physical system is directly or indirectly dependent on surrounding temperature or its own temperature, so it is very necessary to study about temperature before working on any system. Temperature measurement can be done by temperature sensors. These temperature sensors when coupled with the control unit, can control other parameters of the system like, in a fire safety control system in a building, a temperature sensor is installed to sense the temperature in the building, if the temperature increase above a critical temperature set, it will send signal to the control unit and can activate a fire safety program. Now a day's temperature sensor device is a very essential part of every machine. And machines are now reducing their size with increasing research and technology. So it is necessary to develop a temperature sensor device with easy and simple structure, high sensitivity, precise, easy to install, and inexpensive.

- **Types of Temperature sensor**

Several sensor devices have been developed to measure temperature in the past. Based on these data temperature sensor are modified to use them in recent technologies.

a) Resistance Temperature Detectors (RTDs)

This device contains a thin film sealed in glass core and a wire wrapped around it, when the sealed metal temperature rises it increases the resistance of the wire, the higher the temperature higher will be the temperature[52-54]. Copper, Nickel, and Platinum are preferred as the metal material. Higher precision can be obtained by using Platinum so it is sometimes called as PRTs[55].

b) Thermistors

This temperature sensor is basically a temperature dependent resistor. Derived its name from two words, THERMal-resiSTORS. Based on its dependency on temperature this resistors can be classified into 2 types as shown in figure 6.1:

- NTC (Negative Temperature Coefficient)

NTC thermistors are those devices in which Resistance of the material decreases with an increase in Temperature.

- PTC (Positive Temperature Coefficient)

PTC thermistors are those devices in which Resistance of the material increases with an increase in Temperature.

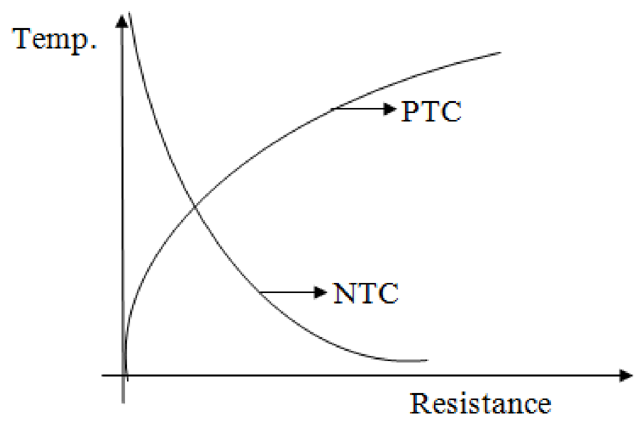

Figure 6.1. Temperature V/s Resistance graph for thermistors

Thermistors have very high sensitivity. Generally, in Temperature sensing, NTC thermistors are used while PTC is used for electric current control [55].

c) Thermocouples

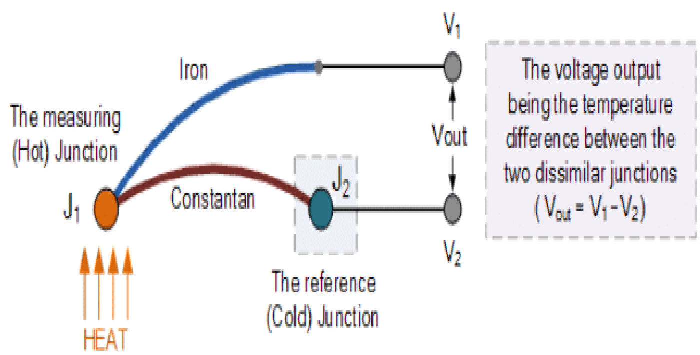

Figure 6.2. Setup of Thermocouple

Two dissimilar metal wires are joined together at one end, generating a thermoelectric voltage at the other open end based on the temperature difference between the 2 metal wires. This device uses the Seebeck effect as the principle. Thermocouples are shown in figure 6.2.

d) Semiconductor Thermometer Devices

Using the fact that semiconductors have I-V characteristics which depend upon Temperature. But these devices are used very less due to small temperature range. But they are accurate and inexpensive.

2. Comparision of Different temperature sensors

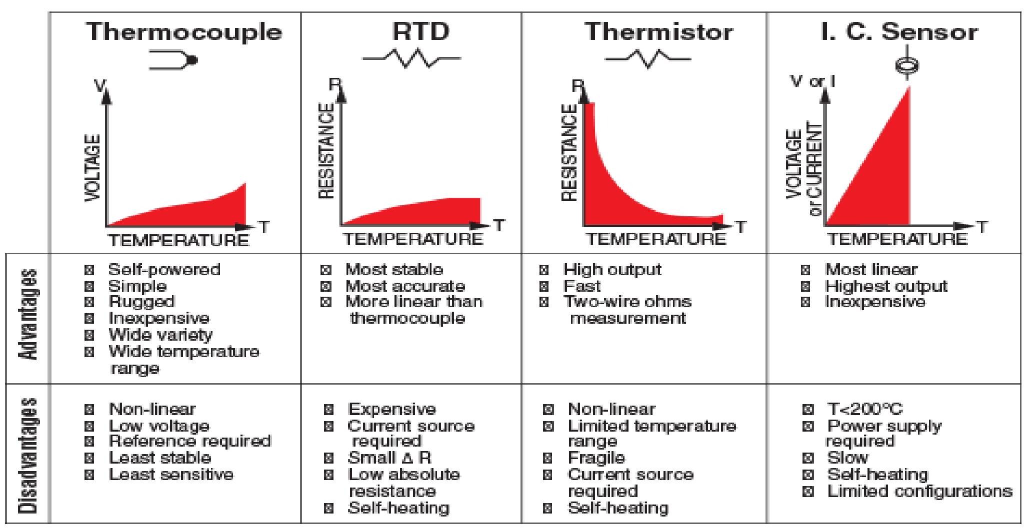

Figure 6.3. Advantage disadvantages of the different temperature sensor.

Different temperature sensors have different temperature sensing principles so they also have advantage and disadvantage when compared to each other as shown in Figure 6.3.

3. ZnO and Mn doped ZnO for temperature sensor

The semiconductor material is the most promising material for temperature sensing [56, 57]. It has very useful properties, so it can be used as a temperature sensor material [57]. Though we have not found any literature for Mn doped ZnO temperature sensor, in the previous chapter of this thesis it was found that properties of ZnO are changing with Mn, so we have decided to study the effect of Mn doped ZnO on its ZnO based Temperature Sensor.

4. Fabrication of Thermistors and Setup of the temperature sensor

In this section, we have used the previously fabricated samples for thermistor application. For making device, these samples were cut into 1x1 cm^2 and Silver paste is used to make point contacts at the diagonal of these devices for conduction. These samples were then encased in a heating chamber and point contact of samples were connected to Keithley 2401 sourcemeter as shown in figure 6.4, for calculation of Voltage and Resistance, and Temperature is then increased and its variation with Resistance is seen at different Voltage. We have chosen Voltage = 0.1V, 0.2V, 0.5V, 1V, 2V and T= 25 ^oC, 50 ^oC, 100 ^oC, 150 ^oC, 200 ^oC, 250 ^oC, 300 ^oC, 350 ^oC, 400 ^oC. Labview software is used to perform the experiment in Keithley 2401 sourcemeter.

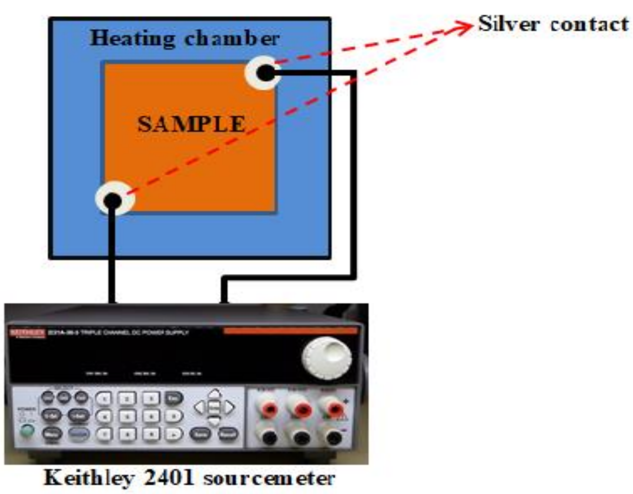

Figure 6.4. Experimental setup for the temperature sensor.

5. Result and Discussion

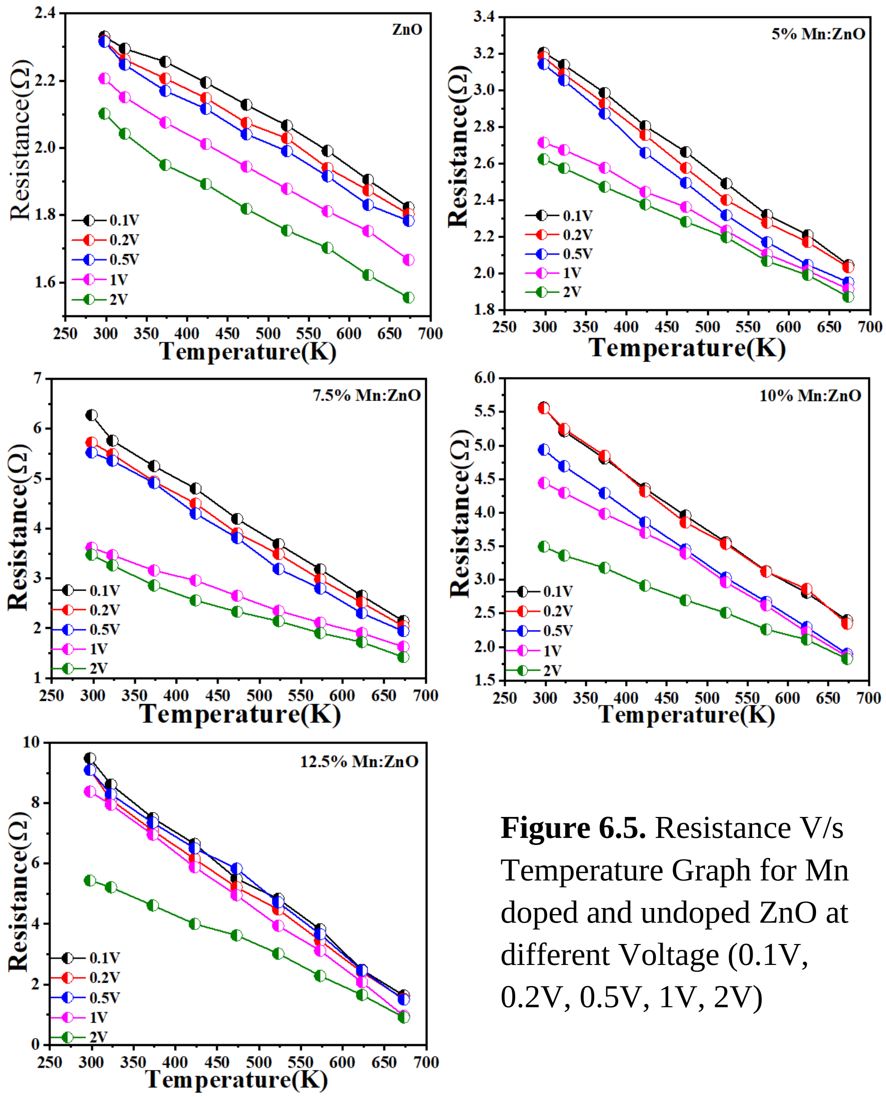

Figure 6.5. Resistance V/s Temperature Graph for Mn doped and undoped ZnO at different Voltage (0.1V, 0.2V, 0.5V, 1V, 2V)

Figure 6.5 shows the variation of Resistance with Temperature at different Voltages for Mn doped and undoped Samples. It can be seen from the figure that for any given voltage, Resistance of the all the samples decreases linearly with an increase in Temperature. Hence it is said to be acting as an NTC thermistor, as also seen by the semiconducting device [58].

- **Temperature Coefficient of Resistance(∝)**

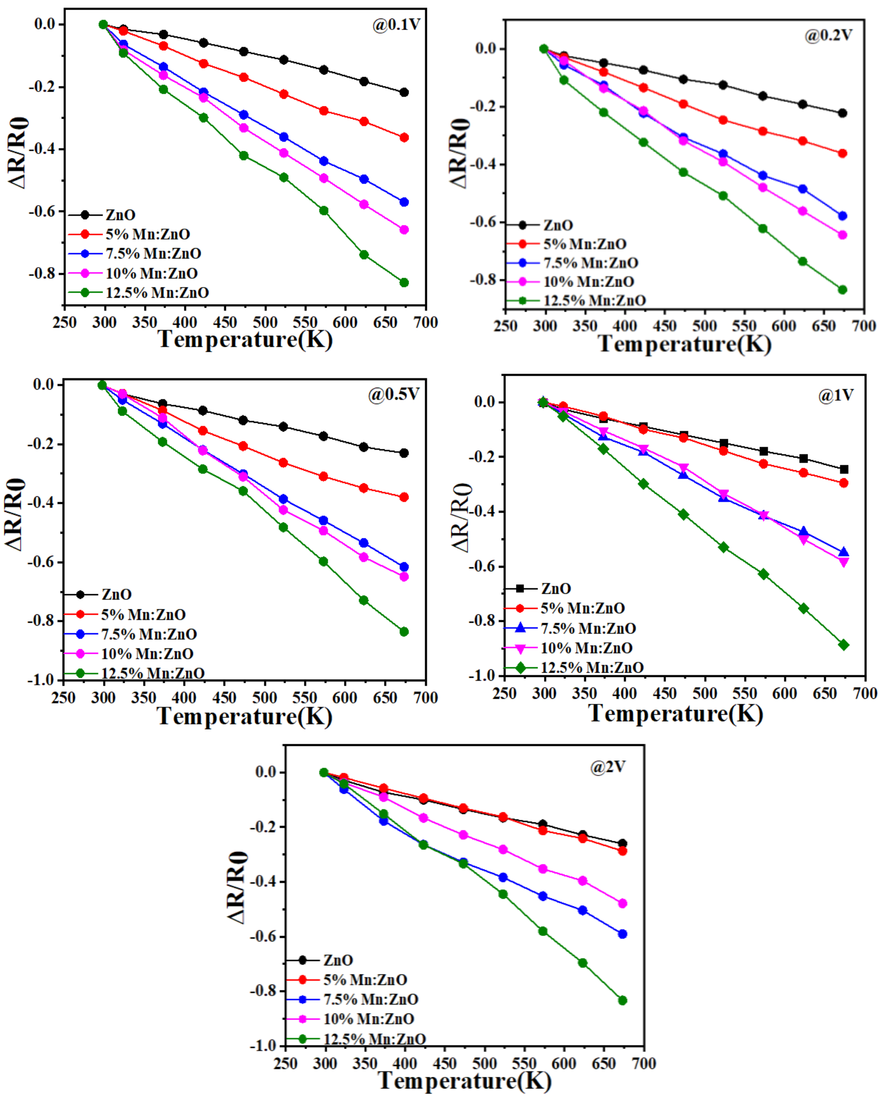

Figure 6.6. Relative change in resistance V/s Temperature graph of Pure and Mn doped ZnO at different Voltage (0.1V, 0.2V, 0.5V, 1V, 2V)

The TCR(∝) of samples can be found out by the following equation 15,

$$\boldsymbol{R(T) = R(T_0)[1 + \alpha\, \Delta T]} \tag{15}$$

Where R(T) is resistance at a given temperature, $R(T_0)$ is resistance at initial temperature (298K), $\propto$ is TCR of the temperature sensor, ΔT is change in temperature (K). A graph can be plotted using the above equation between ($\Delta R/R_0$) V/s T i.e. change in resistance V/s temperature. By liner fitting of this graph, a slope can be estimated which be equal to $\propto$ i.e. TCR. So, a graph has been plotted for change in resistance V/s temperature for all samples at different voltage are as shown in figure 6.6, and the TCR values are estimated using linear fitting of this graph. TCR values for all samples at different temperature are shown in table 4.

Mn doping	0.1V	0.2V	0.5V	1V	2V
0%	-0.571×10^{-4}	-0.576×10^{-4}	-0.596×10^{-4}	-0.625×10^{-4}	-0.667×10^{-4}
5%	-0.977×10^{-4}	-0.975×10^{-4}	-0.810×10^{-4}	-0.805×10^{-4}	-0.756×10^{-4}
7.5%	-1.49×10^{-4}	-1.5×10^{-4}	-1.63×10^{-4}	-1.46×10^{-4}	-1.25×10^{-4}
10%	-1.7×10^{-4}	-1.72×10^{-4}	-1.8×10^{-4}	-1.56×10^{-4}	-1.50×10^{-4}
12.5%	-2.14×10^{-4}	-2.13×10^{-4}	-2.16×10^{-4}	-2.34×10^{-4}	-2.19×10^{-4}

Table 4. Calculated TCR values of Mn doped and undoped ZnO at a different voltage in (K^{-1}).

- **Sensitivity**

The sensitivity of the Temperature sensor can be calculated using equation 16.

$$\boldsymbol{Sensitivity} = \frac{R(T)-R(T_0)}{T-T_0} = \frac{\Delta R}{\Delta T} \qquad (16)$$

Where ΔR is change in resistance and ΔT is change in temperature.

The sensitivity of all samples at different voltage is shown in table 5.

Mn doping	0.1V	0.2V	0.5V	1V	2V
0	0.17045	0.17185	0.17761	0.18654	0.1990
5%	0.29122	0.29058	0.30992	0.24013	0.22539
7.5%	0.44402	0.447	0.48574	0.43508	0.3725
10%	0.5066	0.51256	0.5364	0.46488	0.447
12.5%	0.63772	0.63474	0.64368	0.69732	0.65262

Table 5. Calculated Sensitivity values of Mn doped and undoped ZnO at a different voltage in (ΩK^{-1}).

6. Conclusion

It can be concluded from the above discussion that at a particular voltage, TCR and Sensitivity increases with an increase in Mn doping concentration but a temperature sensor with TCR around 10^{-4} K^{-1} is preferred, our TCR value is also around 10^{-4} K^{-1} for ZnO and 5% Mn doped ZnO and it increased to 10^{-3} K^{-1} for further increase in Mn concentration. We have also seen an increase in sensitivity with Mn doping. So we can say that pure ZnO is a suitable device for temperature sensing application

CHAPTER 7

Summary, Conclusions and Future Scope

The effect of Mn doping in ZnO crystal structure has been studied in detail at a different doping level of 5%, 7.5%, 10%, and 12.5% which were synthesized successfully using a wet chemical approach with is a simple and economical method. Characterization of the samples was done using XRD, SEM, Uv-Vis, TEM, etc. SEM results show that with doping the nanostructure diameter of ZnO reduced to half while increasing the density of nanostructure and changing the structure of ZnO from nanorods flowers to simple nanorods. XRD results show that Mn is successfully incorporated in the ZnO crystal structure increasing the lattice parameter, unit cell Volume and Bond length with an increase in Mn doping concentration, while there is an increase in particle size by incorporation of Mn in ZnO crystal, however further increment of particle size with an increase in Mn concentration is almost negligible. Raman spectroscopy results show an additional broad peak in Mn doped ZnO, depicting that Mn is incorporated in

ZnO and a decrease in Oxygen is also seen from these results. UV-Vis spectroscopy result shows that with an increase in Mn doping the absorbance of ZnO is shifting toward Visible range and also a decrease in band gap from 3.5 eV for ZnO to 3.16 eV for 12.5% Mn doped ZnO makes it a promising material for electronics and optoelectronics devices. PL results show that Oxygen vacancy is increasing with the increase in Mn doping as also seen in Raman spectroscopy while defect related energy levels are created in between valence band and conduction band making it a suitable candidate for Photoluminescence devices.

By fabrication of Temperature sensing device, Thermistor, Temperature sensing application of Mn doped ZnO is studied for the first time, It is seen that ZnO and Mn doped ZnO are NTC resistor means with increase in temperature, resistance of the sensor decreased giving a Negative Temperature Coefficient Resistance (α) of around 10^{-4} K^{-1} and at low voltage (V) the TCR value is, even more, better than higher voltage, making it a material with self-conducting Thermistor. The sensitivity of the material for temperature sensing increased with Mn doping, for ZnO it was around $0.2\Omega K^{-1}$ and for 12.5% Mn doped ZnO was around 0.6 ΩK^{-1}at 2 V. So to get a temperature sensor with high TCR and high sensitivity, less amount of Mn doped ZnO is best for use. In the present thesis, the pure ZnO device shows that it is the best device to use as a temperature sensor.

Conclusions:

- Mn doped ZnO synthesized successfully by the simple and economical wet chemical method by optimizing the synthesis parameters.
- Mn doping in ZnO represents a change in dimension of the nanorods without changing morphology.
- 5 % Mn doped ZnO represents the good candidate for the thermistor applications.

Future scope

Mn doped ZnO is not explored much; however, this will be interesting to check the possible applications as mentioned below:

- In Electronics and optoelectronic devices.
- Study of Magnetic Properties of Mn doped ZnO
- For gas sensing and humidity

References

1. Whatmore, R.W., *Nanotechnology—what is it? Should we be worried?* Occupational Medicine, 2006. **56**(5): p. 295-299.
2. Goddard III, W.A., et al., *Handbook of nanoscience, engineering, and technology*. 2012: CRC press.
3. Wang, Z.L., *Nanostructures of zinc oxide.* Materials today, 2004. **7**(6): p. 26-33.
4. Jeevanandam, J., et al., *Review on nanoparticles and nanostructured materials: history, sources, toxicity and regulations.* Beilstein journal of nanotechnology, 2018. **9**(1): p. 1050-1074.
5. Future Markets, I., *NanoZnO*, in *Future Markets Magazine*. 2014. p. 14.
6. Coleman, V. and C. Jagadish, *Basic properties and applications of ZnO*, in *Zinc oxide bulk, thin films and nanostructures*. 2006, Elsevier. p. 1-20.
7. Morkoç, H. and Ü. Özgür, *Zinc oxide: fundamentals, materials and device technology*. 2008: John Wiley & Sons.
8. Espitia, P.J.P., et al., *Zinc oxide nanoparticles: synthesis, antimicrobial activity and food packaging applications.* Food and Bioprocess Technology, 2012. **5**(5): p. 1447-1464.
9. Tuomisto, F., et al., *Introduction and recovery of point defects in electron-irradiated ZnO.* Physical Review B, 2005. **72**(8): p. 085206.
10. Look, D.C., J.W. Hemsky, and J. Sizelove, *Residual native shallow donor in ZnO.* Physical review letters, 1999. **82**(12): p. 2552.
11. Wang, Z.L., *Zinc oxide nanostructures: growth, properties and applications.* Journal of physics: condensed matter, 2004. **16**(25): p. R829.
12. Fan, Z. and J.G. Lu, *Zinc oxide nanostructures: synthesis and properties.* Journal of nanoscience and nanotechnology, 2005. **5**(10): p. 1561-1573.
13. Porter, F.C., *Zinc handbook: properties, processing, and use in design*. 1991: Crc Press.
14. Subramanyam, T., B. Srinivasulu Naidu, and S. Uthanna, *Physical properties of zinc oxide films prepared by dc reactive magnetron sputtering at different sputtering pressures.* Crystal Research and Technology: Journal of Experimental and Industrial Crystallography, 2000. **35**(10): p. 1193-1202.
15. Jin, Z., et al., *High throughput fabrication of transition-metal-doped epitaxial ZnO thin films: A series of oxide-diluted magnetic semiconductors and their properties.* Applied Physics Letters, 2001. **78**(24): p. 3824-3826.
16. Janotti, A. and C.G. Van de Walle, *Fundamentals of zinc oxide as a semiconductor.* Reports on progress in physics, 2009. **72**(12): p. 126501.
17. Guzmán, M., N. Agulló, and S. Borrós. *Reducing zinc oxide in rubber industry use through the development of mixed metal oxide nanoparticles*. in *The 11th Edition of the Trends in Nanotechnology International Conference (TNT2010),(Braga, Portugal)*. 2010.

18. Kołodziejczak-Radzimska, A. and T. Jesionowski, *Zinc oxide—from synthesis to application: a review.* Materials, 2014. **7**(4): p. 2833-2881.
19. Shaban, M., F. Mohamed, and S. Abdallah, *Production and characterization of superhydrophobic and antibacterial coated fabrics utilizing ZnO nanocatalyst.* Scientific reports, 2018. **8**(1): p. 3925.
20. Liu, J., et al., *Migration and characterization of nano-zinc oxide from polypropylene food containers.* Am. J. Food Technol, 2016. **11**: p. 159-164.
21. Rana, A.K., et al., *Studies on the control of ZnO nanostructures by wet chemical method and plausible mechanism.* AIP Advances, 2015. **5**(9): p. 097118.
22. Das, R., et al., *Effect of growth temperature on the optical properties of ZnO nanostructures grown by simple hydrothermal method.* RSC Advances, 2015. **5**(74): p. 60365-60372.
23. Vladut, C.M., et al., *Optical and Piezoelectric Properties of Mn-Doped ZnO Films Deposited by Sol-Gel and Hydrothermal Methods.* Journal of Nanomaterials, 2019. **2019**.
24. Yang, S. and Y. Zhang, *Structural, optical and magnetic properties of Mn-doped ZnO thin films prepared by sol–gel method.* Journal of Magnetism and Magnetic Materials, 2013. **334**: p. 52-58.
25. Omri, K., et al., *Magnetic and optical properties of manganese doped ZnO nanoparticles synthesized by sol–gel technique.* Superlattices and Microstructures, 2013. **60**: p. 139-147.
26. Ningsih, S., et al. *Synthesis and Characterization of ZNO/MN Nanocomposite by using Sol-Gel Method*. in *IOP Conference Series: Materials Science and Engineering*. 2018. IOP Publishing.
27. Sabri, N.S., A.K. Yahya, and M.K. Talari, *Emission properties of Mn doped ZnO nanoparticles prepared by mechanochemical processing.* Journal of luminescence, 2012. **132**(7): p. 1735-1739.
28. Dhanshree, K. and T. Elangovan, *Synthesis and characterization of ZnO and Mn-doped ZnO nanoparticles.* International Journal of Science and Research, 2015. **4**(11): p. 1816-1820.
29. Jayakumar, O., et al., *Magnetism in Mn-doped ZnO nanoparticles prepared by a co-precipitation method.* Nanotechnology, 2006. **17**(5): p. 1278.
30. Tan, T.L., C.W. Lai, and S.B. Abd Hamid, *Tunable band gap energy of Mn-doped ZnO nanoparticles using the coprecipitation technique.* Journal of Nanomaterials, 2014. **2014**: p. 1.
31. Abdollahi, Y., et al., *Synthesis and characterization of Manganese doped ZnO nanoparticles.* International Journal of Basic & Applied Sciences, 2011. **11**(4): p. 62-69.
32. Binapani Goswami, R.S., *Effect of Mn Doping on Optical Properties of ZnO Nanoparticles.* International Journal of Innovative Research in Science,Engineering and Technology, 2015. **4**(4): p. 6.
33. Sanatombi, S. and I. Soibam, *SYNTHESIS OF MANGANESE SUBSTITUTED ZINC OXIDE BY CHEMICAL CO-PRECIPITATION METHOD.*

34. Shukla, M., *Investigations on the Infuence of Aspect Ratio and Morphology of Hydrothermally Grown ZnO Based Nanostructures Towards Biosensing Applications*, in *Indian Institute of Technology*. 2018, IIT,Indore: Indore.
35. Areef Billah, A., *Investigation of multiferroic and photocatalytic properties of Li doped BiFeO3 nanoparticles prepared by ultrasonication.* 2016.
36. Tighineanu, I., et al., *Porous III-V Semiconductors*. 2005: Ştiinţa.
37. Ismail, K., *FABRICATION AND CHARACTERIZATION OF SURFACE-ENHANCED RAMAN SCATTERING SUBSTRATES THROUGH PHOTO-DEPOSITION OF GOLD NANOPARTICLES.* 2015.
38. Hasanuzzaman, M., et al., *Properties of glass materials.* Reference Module in Materials Science and Materials Engineering, 2016.
39. Kohli, R. and K.L. Mittal, *Developments in Surface Contamination and Cleaning-Vol 2: Particle Deposition, Control and Removal*. 2009: William Andrew.
40. Schneller, T., et al., *Chemical solution deposition of functional oxide thin films*. 2013: Springer.
41. Hodes, G., *Chemical solution deposition of semiconductor films*. 2002: CRC press.
42. Thein, M.T., et al., *The role of ammonia hydroxide in the formation of ZnO hexagonal nanodisks using sol–gel technique and their photocatalytic study.* Journal of Experimental Nanoscience, 2015. **10**(14): p. 1068-1081.
43. Rana, A.K., et al., *Search for origin of room temperature ferromagnetism properties in Ni-doped ZnO nanostructure.* ACS applied materials & interfaces, 2017. **9**(8): p. 7691-7700.
44. Kumar, Y., et al., *Controlling of ZnO nanostructures by solute concentration and its effect on growth, structural and optical properties.* Materials Research Express, 2015. **2**(10): p. 105017.
45. Strelchuk, V., et al., *Raman submicron spatial mapping of individual Mn-doped ZnO nanorods.* Nanoscale research letters, 2017. **12**(1): p. 351.
46. Russo, V., et al., *Multi-wavelength Raman scattering of nanostructured Al-doped zinc oxide.* Journal of Applied Physics, 2014. **115**(7): p. 073508.
47. Fabbiyola, S., et al., *Structural, microstructural, optical and magnetic properties of Mn-doped ZnO nanostructures.* Journal of Molecular Structure, 2016. **1109**: p. 89-96.
48. Kong, Y., et al., *Ultraviolet-emitting ZnO nanowires synthesized by a physical vapor deposition approach.* Applied Physics Letters, 2001. **78**(4): p. 407-409.
49. ZENG, H., et al., *Violet photoluminescence from shell layer of Zn.* Applied physics letters, 2006. **88**(17).
50. Srivastava, T., et al., *Opto-electronic properties of Zn (1-x) VxO: Green emission enhancement due to V4+ state.* Journal of Applied Physics, 2017. **122**(2): p. 025106.
51. Lin, J.-H., et al., *Photoluminescence mechanisms of metallic Zn nanospheres, semiconducting ZnO nanoballoons, and metal-semiconductor Zn/ZnO nanospheres.* Scientific reports, 2014. **4**: p. 6967.
52. Prost, W., et al., *High performance III/V RTD and PIN diode on a silicon (001) substrate.* Applied Physics A, 2007. **87**(3): p. 539-544.

53. Kim, J., et al., *A study on the fabrication of an RTD (resistance temperature detector) by using Pt thin film.* Korean Journal of Chemical Engineering, 2001. **18**(1): p. 61-66.
54. Sen, S.K., *An improved lead wire compensation technique for conventional two wire resistance temperature detectors (RTDs).* Measurement, 2006. **39**(5): p. 477-480.
55. Yadav, B., et al., *Temperature sensors based on semiconducting oxides: An overview.* arXiv preprint arXiv:1205.2712, 2012.
56. Yadav, B. and A. Yadav, *Synthesis of nanostructured cuprous oxide and its performance as humidity and temperature sensor.* International Journal of Green Nanotechnology: Materials Science & Engineering, 2009. **1**(1): p. M16-M31.
57. Chang, J., et al., *The effects of thickness and operation temperature on ZnO: Al thin film CO gas sensor.* Sensors and actuators B: Chemical, 2002. **84**(2-3): p. 258-264.
58. Neella, N., et al. *Negative temperature coefficient behavior of graphene-silver nanocomposite films for temperature sensor applications*. in *2016 IEEE 11th Annual International Conference on Nano/Micro Engineered and Molecular Systems (NEMS)*. 2016. IEEE.